[redacted]

COPY # 1 OF 14 COPIES
THIS DOCUMENT CONTAINS 122 PAGES

T-59

FUNDAMENTAL DESIGN PRINCIPLES OF AN ATTACK SIMULATOR FOR AIRBORNE FIRE CONTROL SYSTEMS

by
R. C. Duncan

May, 1954

GROUP - 4
Downgraded at 3 year intervals;
declassified after 12 years.

[redacted]L

Unclassified per DoD dir 5200.10 dtd. 3/31/64 as of 6/14/66

[redacted]

FUNDAMENTAL DESIGN PRINCIPLES OF AN ATTACK SIMULATOR FOR AIRBORNE FIRE CONTROL SYSTEMS

by

Robert C. Duncan, Lieutenant, U.S. Navy
B.S., U.S. Naval Academy, 1945
B.S. (Aeronautical Engineering)
U.S. Naval Postgraduate School, 1953

SUBMITTED IN PARTIAL FULFILLMENT OF THE
REQUIREMENTS FOR THE DEGREE OF
MASTER OF SCIENCE
at the
MASSACHUSETTS INSTITUTE OF TECHNOLOGY
1954

Signature redacted

Signature redacted

Signature of Author ______________________
Dept. of Aeronautical Engineering, May 24, 1954

Signature redacted

Signature redacted

Certified by ______________________
Thesis Supervisor

Signature redacted

____
Chairman, Departmental Committee on Graduate Students

[redacted]

CONFIDENTIAL

NOTICE

This document contains information affecting the National defense of the United States within the meaning of the Espionage Laws, Title 18, U.S.C., Sections 793 and 794. Its transmission or the revelation of its contents in any manner to an unauthorized person is prohibited by law.

This thesis, written by the authors while affiliated with the Instrumentation Laboratory, M.I.T., has been reproduced by the offset process using printer's ink in accordance with the following basic authorization, received by Dr. C.S. Draper, Director of the Instrumentation Laboratory.

COPY

April 7, 1950

Dr. C.S. Draper
33-103

Dear Dr. Draper:

Mr. L.E. Payne has shown to me a recent printed reproduction of a thesis, in this instance a Master's dissertation, submitted in partial fulfillment of the requirements for the degree of Master of Science at the Massachusetts Institute of Technology.

The sample shown is printed by the offset press using screened illustrations, graphs and other material. For the purposes of the Library which include record and permanent preservation, theses reproduced in this manner are perfectly satisfactory and in my opinion meet all of the physical requirements of the graduate school insofar as they pertain to the preparation of a thesis.

I note that in the sample submitted the signatures have been reproduced along with the text by photo lithography. It is suggested that for the Library record copy the author, thesis supervisor and chairman of the Departmental Committee on Graduate Students affix their signatures in writing as complete authorization of the study. These can be written above the reproduced signature if desired.

Sincerely yours,

(signed)

Vernon D. Tate
Director of Libraries

VDT/jl

cc: Dean Bunker
Mr. Payne

COPY

FUNDAMENTAL DESIGN PRINCIPLES OF AN ATTACK SIMULATOR FOR AIRBORNE FIRE CONTROL SYSTEMS

by

Robert C. Duncan

Submitted to the Department of Aeronautical Engineering on May 24, 1954, in partial fulfillment of the requirements for the degree of Master of Science in Aeronautical Engineering.

ABSTRACT

An evaluation system incorporating an Attack Simulator as an integral unit was proposed in this thesis as a method of overcoming the deficiencies of present methods of in-flight evaluation of the dynamic performance characteristics of airborne fire control systems.

The basic concepts of programming as input quantities to the Attack Simulator either target space motion or angular velocity of the line of sight were compared with respect to the complexity of the resulting Attack Simulator functional design.

It was shown that an Attack Simulator can be built as a practical system within the scope of modern design capabilities. It was shown that the Attack Simulator would most effectively take the form of an airborne installation to activate the tracking components of the fire control system by programming angular velocity of the line of sight to the target as input command signals to a stabilized platform in the interceptor aircraft.

Thesis Supervisor: Walter Wrigley

Title: Associate Professor of Aeronautical Engineering

May 24, 1954

Professor Leicester F. Hamilton
Secretary of the Faculty
Massachusetts Institute of Technology
Cambridge 39, Massachusetts

Dear Professor Hamilton:

In accordance with the regulations of the faculty, I hereby submit a thesis entitled Fundamental Design Principles of An Attack Simulator for Airborne Fire Control Systems in partial fulfillment of the requirements for the degree of Master of Science in Aeronautical Engineering.

Signature redacted

Robert C. Duncan

ACKNOWLEDGEMENT

The author expresses his appreciation to the personnel of the Instrumentation Laboratory, Massachusetts Institute of Technology who assisted in the preparation of this thesis. Particular thanks are due to

Dr. W. Wrigley, who, as thesis supervisor inspired and guided the entire project.

Mr. John A. Gautraud for his interest, encouragement, willingness to discuss the project at any time regardless of personal commitments, and for setting an example of great technical skill.

Mr. R. W. Gras and Mr. L. A. Riley for their help in the theoretical and practical aspects of the fire control problem.

The graduate work for which this thesis is a partial requirement was performed while the author was assigned to the Naval Administrative Unit, Massachusetts Institute of Technology.

TABLE OF CONTENTS

OBJECT

The object of this thesis is to determine a practical method of simulating in flight the air-to-air attack problem for interceptor aircraft. It is also the object of this thesis to simulate the attack problem with sufficient realism that the dynamic characteristics of fire control systems under development may be evaluated by techniques and in ranges of operation beyond the scope of present in-flight test procedures.

CHAPTER 1

INTRODUCTION

At an advanced stage in the evolution of the new automatic equipment for aircraft, particularly complete systems such as a closed loop fire control system, it is desirable that the equipment be subjected to tests closely approximating the conditions under which it is designed to operate. Often, it is desired to compare the performance of the system with various modifications of the individual components in order to determine that configuration which gives optimum performance characteristics under expected operating conditions.

1.1 Limitations of Evaluating Fire Control System Performance from Firing Runs

One obvious method of evaluating the performance of fire control systems in combination with real aircraft and real tracking systems is for an aircraft in which the equipment is installed to make firing runs against towed targets or drones. The speeds, altitudes, and maneuvers of the target by this method are severely limited; hence the operating conditions of the system under test may differ greatly from those to which it would be subjected in a combat environment. Evaluation of the system by this procedure depends primarily on a determination of the percentage of hits achieved. However, this method provides no information about the time variation of dynamic errors in the system during the attack run. It is difficult to compare the performance of different modifications of the equipment since the initial conditions of the attack problem for any two runs cannot be made the same.

1.2 Limitations of Evaluating Fire Control System Performance by Reproducing the Attack Run on the Ground from Data Recorded in Flight

In one type of an evaluating program conducted today, a series of attack runs is made by an interceptor on a target aircraft. During the attack runs, data is recorded on the motion of the two aircraft in order that the run may be reproduced on the ground to determine the time variation of dynamic errors in the fire control system during the attack run. In order ro reproduce the attack run on the ground, it is necessary to measure at various fixed times or continuously:

(1) The position of the interceptor with respect to the target.

(2) The angular orientation of the interceptor with respect to the target.

(3) The true airspeeds of the two aircraft.

The position in space of the interceptor relative to the target is determined by direct measurements of range and target angle during the attack run.

(1) Range is recorded on an oscillograph from the radar in the interceptor.

(2) Target angle is measured by an observor in a rear sighting station of the target airplane. The observor continuously tracks the interceptor during the attack run. To facilitate this tracking, an azimuth ring is fixed to the target airplane and a pointer is fixed to the sighting station. Movies are made of the relative position of the pointer with respect to the target airplane during the attack run from which target angle can be continuously determined.

The angular orientation of the interceptor relative to the target is determined either by a boresighted camera in the front cockpit of the interceptor or a recording of radar antenna gimbal angles. The interceptor roll angle is determined either by measuring the angular orientation of the interceptor with respect to the horizon in the photographs from the boresighted camera, or from a roll integrating gyro in the interceptor. Evaluation by boresighted camera techniques is limited to the camera's field of vision.

Airspeeds of target and interceptor are normally limited to constant speeds in order to simplify data reduction. For runs in which the speeds of either are varied, it is necessary to record continuously the indicated airspeeds and convert to true airspeeds at the altitudes in question.

In order to compute from the data that is recorded, it is necessary that all records have a common time reference. The recording equipment is located at widely different stations in two separate airplanes. Time synchronization is difficult under such conditions.

The evaluation procedure discussed here requires difficult data reduction techniques. The measurements recorded in flight may be quite approximate due to the inherent accuracy limitations of the equipment used. Hence, answers based on these quantities may often by inaccurate to the point of being unacceptable.

The procedure is expensive in terms of both time and money. Two aircraft must be suitably modified to carry the recording equipment. The aircraft may be needed for many flight hours because much time is required after each run to jockey the target and interceptor into position before commencing the next run. The expense of the aircraft goes beyond the cost of the fuel and men required to fly them; many man-hours of ground maintenance are necessary for each hour in flight.

1.3 Requirements of the Evaluation Program

It is highly desirable that an in-flight evaluation system be developed to provide:

(1) More efficient and greatly simplified flight testing procedures.

(2) The capability of repeating attack runs under identical initial conditions at target acquisition.

(3) Simplified data reduction requirements. In order to conduct the most efficient flight test evaluation program, it is valuable to know quickly the results of one series of flights in order that the next series of flights may be

programmed to provide information in critical performance regions of the equipment being tested.

1.4 The Attack Simulator

An evaluation system incorporating an Attack Simulator as an integral unit was proposed in this thesis as one method of overcoming the shortcomings of present evaluation techniques.

An Attack Simulator as defined in this thesis was considered to be a complete and self-contained system to set up attack problems for an interceptor aircraft in flight such that:

(1) Tracking information on a fictitious target is continuously provided during the attack run to activate the fire control system of the interceptor aircraft.

(2) Sufficient data is continuously recorded from which the performance characteristics of the fire control system can be determined.

(3) Arbitrary initial conditions at target acquisition may be repeated.

CHAPTER 2

DISCUSSION OF RESULTS

2.1 Procedure

The procedure followed in this thesis consisted essentially of an investigation of:

(1) Functional design of an Attack Simulator that programs target space path. This design requires measured quantities be fed back from the interceptor aircraft that indicate the response of the fire control system and aircraft to the attack problem.

(2) Functional design of an Attack Simulator that programs angular velocity of the line of sight. This design does not incorporate quantities that are fed back except the physical orientation of the interceptor aircraft in space.

The studies of phase (1) above were performed in three parts:

(1) The determination of functional design requirements of the Attack Simulator when the attack problem is represented in its complete form as a three-dimensional space relationship of target, interceptor, and projectile trajectory.

(2) An investigation into simplifications possible in the functional design if the ballistic characteristics of the projectile were such that gravity and air drag had no effect on the trajectory. It was assumed here that the projectiles traveled in a straight line in the direction fired at a constant velocity from the instant of firing to impact. This, in effect, restricted the attack problem to the kinematic three-dimensional problem. It was assumed here that the ballistic components of the fire control system could be suitable deactivated to make evaluation under

these conditions possible.

(3) An investigation was made of further simplifications in the functional design of the Attack Simulator if the attack problem were restricted to horizontal two-dimensional space.

The analysis of phase (2) was performed in two parts:

(1) An investigation into a simplified Attack Simulator design that has as its primary function of the activation of the tracking components of the fire control system.

(2) An investigation into methods of expanding this form of the Attack Simulator into a system that provides useful evaluation information about the dynamic performance characteristics of the fire control system.

2.2 Results

The results of the investigation performed in this thesis were considered to be adequate proof that it is possible to design and build a practical Attack Simulator system. It was concluded, furthermore, that a program to build such a system should be undertaken in view of the need for it as an evaluation instrument and the feasibility of it as a practical system within the scope of modern design capabilities.

It was shown in this thesis that an Attack Simulator in which every known or measurable factor in the attack problem is included would require a system that is intricate and complex. It was indicated that such a system may take the form of a ground installation with

(1) Target information telemetered to the interceptor aircraft to activate the fire control system.

(2) Measurements of interceptor motion and fire control system output quantities telemetered from the aircraft to the ground.

It was shown in this thesis, however, that the Attack Simulator would most effectively take the form of an airborne installation.

It was shown that an Attack Simulator in which the kinematic attack problem alone is considered would be greatly simplified in design and would provide accurate evaluation data on all parts of the fire control system except the ballistics section of the computer.

It was demonstrated in this thesis that Attack Simulator design may be simplified by restricting the attack problem to a single horizontal plane. Inaccuracies were discussed that result from assuming the interceptor path remained in the horizontal plane throughout any attack in which the target is restricted to the altitude of the interceptor at the start of the problem.

It was concluded in this thesis that the only reasonable from an Airborne Attack Simulator could take in view of the size and weight limitations imposed on equipment installed in interceptor aircraft* would be one in which the computations required of the Attack Simulator are restricted to an absolute minimum. Furthermore, it was concluded that the complexity of the system could only be reduced sufficiently by departing from the concept of defining precisely the motion of the fictitious target in space to the concept of programming angular velocity of the line of sight based on typical variations in lead pursuit attacks under prescribed initial conditions.

It was concluded in this thesis that an Airborne Attack Simulator that serves as no more than a tracking system activation unit would be a valuable evaluation instrument in early test stages of new fire control systems. It was shown that this simplified from of the Attack Simulator may take the form of a platform mounted on three gimbals with three integrating gyros properly orientated on the platform. The motion of the interceptor aircraft, which serves as the base of the platform, may be isolated such as to stabilize the platform in space. A line in the platform may represent the line of sight to the target and it may be moved in space by programmed command signals proportional to the desired line of sight angular movement. The fire control system may be activated by a signal proportional to the difference in angular displacement of the gimbals at the radar and those of the tracking activation unit. This quantity is tracking line error.

It was shown that refinements are possible in the tracking activation system described briefly above to provide order of magnitude information on the dynamic performance characteristics of the fire

---

* It is generally accepted by aircraft designers that, because of structural and other considerations, modern aircraft are 9 to 15 pounds heavier for each pound of equipment added to the airplane.

control system in response to the attack problem. It was shown that this evaluation system would take the form of simultaneous programmed inputs of line of sight angular velocity, present range, and correct controlled line angular velocity. These programmed inputs may be modified by fed back measurements of interceptor motion in order to make the target follow more closely the same space path for successive attack runs.

It was concluded that a practical Airborne Attack Simulator program would consist of:

(1) Detailed design and construction of the tracking activation form of the Attack Simulator described in this thesis.

(2) Expansion of the tracking activation system into an accurate evaluation system by incorporating simultaneous programmed inputs. These inputs may be modified by quantities fed back from the interceptor.

CHAPTER 3

CONCLUSIONS

1. The Attack Simulator is a needed and practical system for the evaluation of the performance characteristics of modern fire control systems in flight.

2. The Attack Simulator would most effectively be an airborne installation in the interceptor aircraft.

3. The Attack Simulator should be restricted to the kinematic attack problem.

4. The complexity of the attack problem is such that the Attack Simulator should be designed with the concept of programming angular velocity of the line of sight rather than the concept of programming target motion in space.

5. The Airborne Attack Simulator may take the form of a unit designed simply to activate the tracking components of the fire control system. This is a baluable evaluation instrument relatively simple in design and inexpensive to construct.

6. The tracking activation form of the Airborne Attack Simulator would most effectively consist of a stabilized platform in the interceptor. This platform is moved in space by programmed command signals proportional to the desired line of sight angular movement.

7. The first phase of a building program for the Attack Simulator should take the form of the tracking activation unit of (6) above.

8. Successive attack runs in which it is desired to repeat the initial conditions of the attack problem are within the scope of the system of (6).

9. Refinements are possible in the simplified Attack Simulator

of (6) to make available quantitative information on the dynamic characteristics of the fire control system during the attack problem. Successive attack runs in which it is desired to have the fictitious target follow the same space path are possible by feeding back measurements of interceptor motion.

CHAPTER 4

RECOMMENDATIONS FOR FUTURE INVESTIGATIONS

1. The particular form of Attack Simulator described in this thesis consisting of a unit to activate the tracking components of the fire control system should be built and installed in an interceptor aircraft as the first approach toward a useful Attack Simulator evaluation system. This could be done as a special application of the stable platform used in the Black Warrior Fire Control System under development at the Massachusetts Institute of Technology Instrumentation Laboratory.

2. Studies should be undertaken to determine how near the lead pursuit space path flown by an interceptor under the conditions of the kinematic attack problem is to the lead pursuit path in response to the complete fire control problem.

3. Detailed study should be made of the departure from the horizontal plane of an interceptor in the kinematic lead pursuit attack if the target and interceptor are initially in the same horizontal plane and if the target remains in this horizontal plane throughout the attack problem. The results of this investigation may be expanded to show the inaccuracies resulting from the $D_{(LS)_o} = 0$ assumption made in this thesis in the consideration of the horizontal two-dimensional problem.

4. An investigation should be undertaken of the accuracy with which the dynamic characteristics of the fire control system can be evaluated under normal flight conditions when the angular velocity of the line of sight, present range, and correct controlled line angular velocity are simultaneously programmed for typical lead pursuit

attacks under prescribed initial conditions and prescribed target space path and speed.

CHAPTER 5

SIMULATING THE AIR-TO-AIR ATTACK PROBLEM

5.1 The Interceptor Fire Control Problem

The armed interceptor airplane is an important unit in the continental defense system of the United States. The interceptor attack problem commences in its broadest sense at the instant an unidentified air target is picked up by the long range search radar guarding the approaches to the continent. The attack problem ends with the destruction of the target.

When an inbound air target is picked up by radar on the ground, the interceptor is vectored into close proximity with the target on the basis of information received from a computer. Upon nearing the target, radar in the interceptor aircraft searches for, then acquires, signals from the target. In this thesis, investigation is made into that phase of the interceptor attack from the time of target acquisition by the airborne fire control system to the time the attack run is broken off.

The interceptor must be positioned relative to the target and orientated in such a direction that any projectile fired will arrive at a point in space coincident with the arrival of the target at that point. The fire control system carried by the interceptor computes future positions of the target by a measurement of the relative motion of the interceptor and target. Relative motion information for the fire control system is provided by the radar in the form of range and bearing to the target. Fig. 5-1 shows quantities that must be computed by the fire control system before the correct space orientation required of the interceptor can be prescribed.

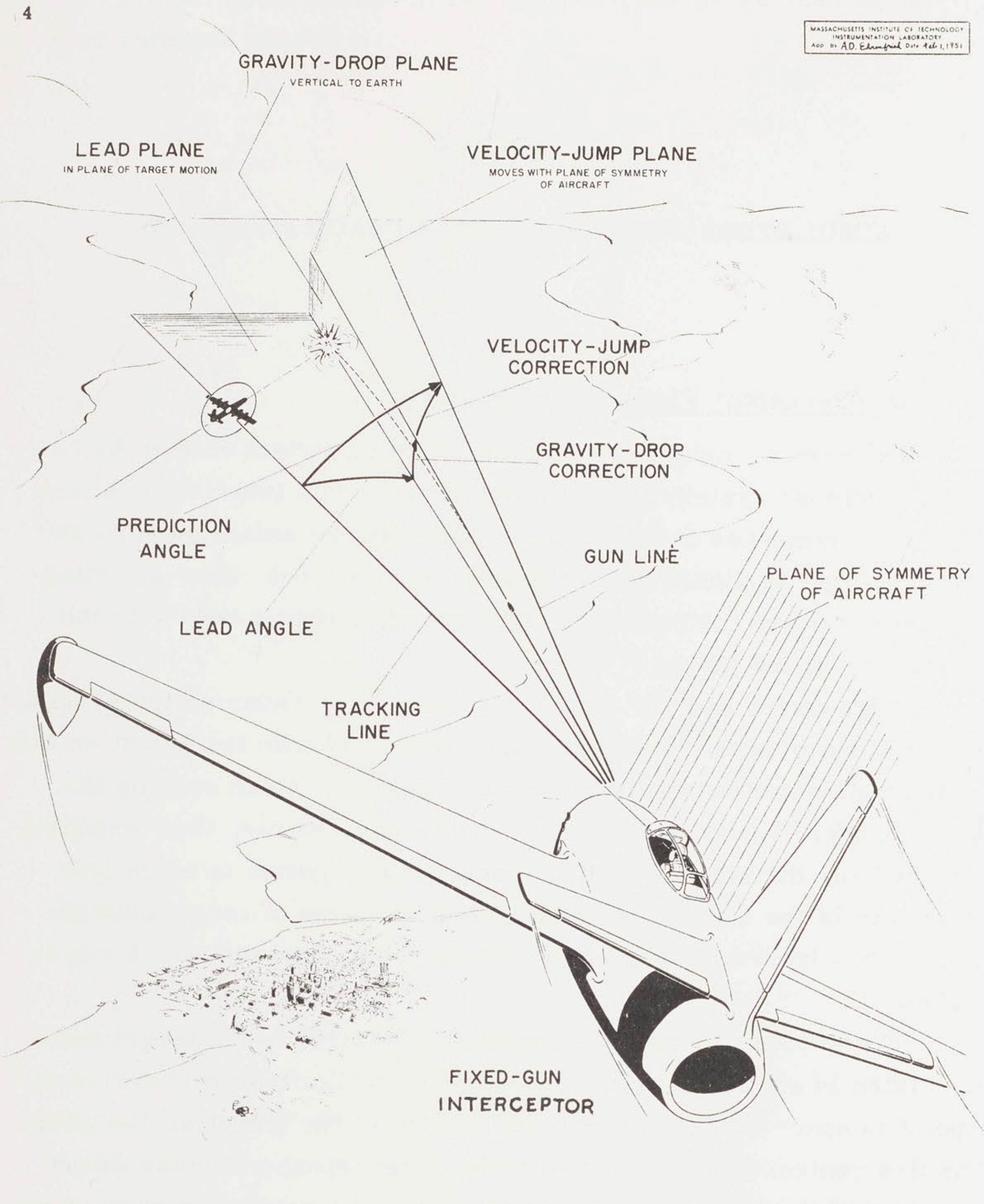

Fig. 5-1 Corrections generated by the Interceptor Fire Control System

The interceptor air-to-air fire control problem is a three-dimensional space relationship of target, interceptor, and projectile trajectory. Equations defining this relationship were derived in Appendix C of this thesis. In these equations, the fire control problem is limited only to the extent that the target remains in one horizontal plane throughtout the attack run. No restrictions are placed on the speed of the target and on changes in heading.

5.2 Operations Required to Simulate the Attack Problem

The interceptor attack problem may be simulated by positioning a fictitious target in space to activate the fire control system of the interceptor. The dynamic performance characteristics of the fire control system may be determined during the attack by measuring output quantities of the fire control system and comparing them to the correct quantities which may be computed from the geometry of the problem. A system to perform these functions is investigated in this thesis. Such a system is called the Attack Simulator.

The operations required of the Attack Simulator are more complex than those of the fire control system. The Attack Simulator performs the following functions:

1. Sets initial relative space position of target and interceptor.
2. Sets initial speed and heading of the target.
3. Programs space motion of target.
4. Measures space motion of interceptor.
5. Computes relative bearing and range information to activate the fire control system in a manner similar to the way the system is activated with tracking of a real target by the radar.
6. Compares continuously the output of the fire control system with correct quantities generated by the Attack Simulator.

5.3 Fire Control Evaluation System Incorporating the Attack Simulator

Fig. 5-2 is a functional diagram of a fire control evaluation system that incorporates the Attack Simulator.

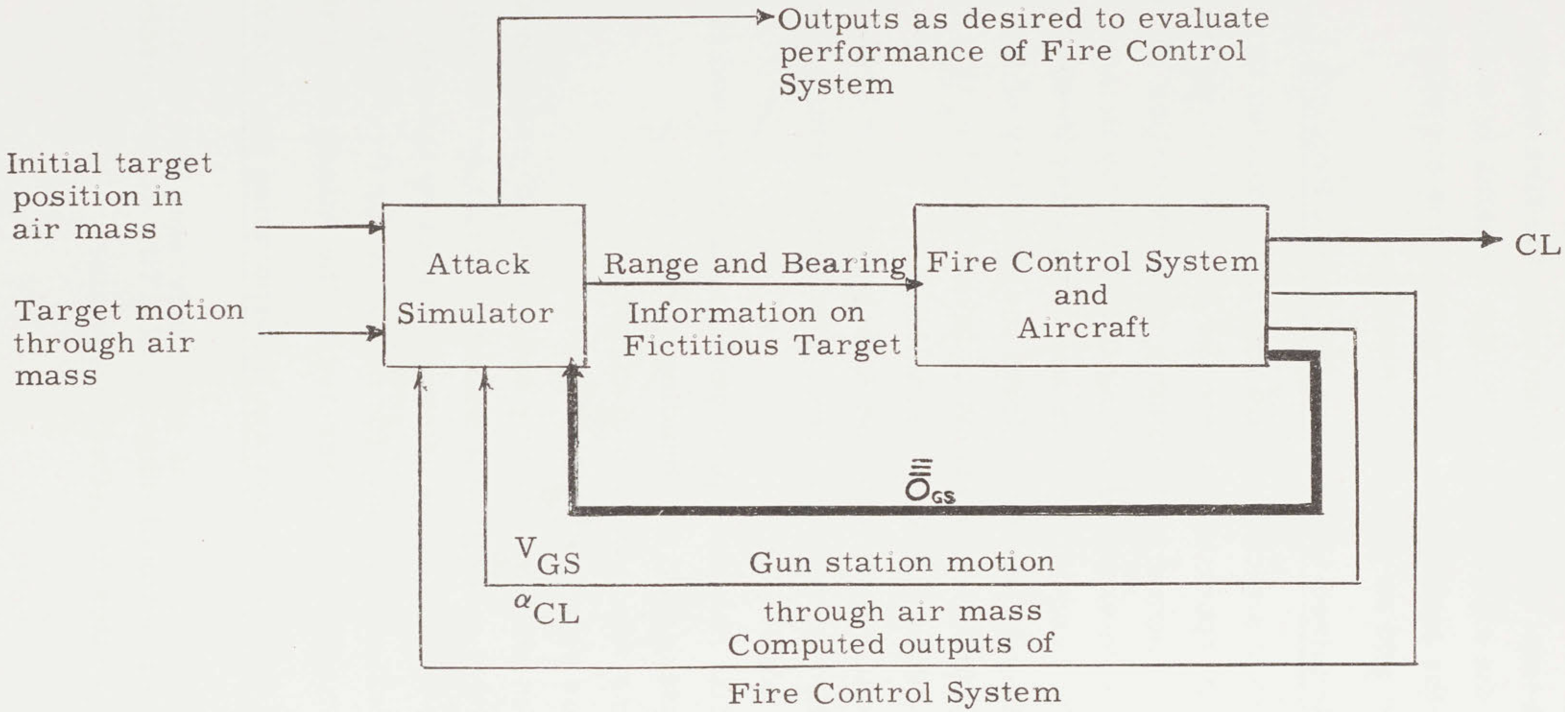

Fig. 5-2 Functional diagram of a fire control evaluation system incorporating the Attack Simulator

CHAPTER 6

FUNCTIONAL DESIGN OF THE ATTACK SIMULATOR

The first phase of the investigations performed in this thesis was the derivation of kinematic and ballistic equations of the fire control problem. The concept of programming the space path of the target in the form of target course and speed through the air mass was considered to be a natural approach to a synthesis of the complete attack problem. It is necessary to examine critically the functional relationship of the equations in order to determine the complexity required of an Attack Simulator that:

1. Is unrestricted in the scope of attack problems it may set up.
2. Provides continuous information to define the correct orientation of the guns in the interceptor.

6.1 Comparison of Reference Frames

The interceptor fire control problem is a short range air-to-air problem. The target and the interceptor both fly in essentially the same air mass, hence it is convenient to consider the fixed reference coordinate system to be the Air Mass Coordinate System. It was shown in Appendix A that the Air Mass Coordinate System X_{AM}, Y_{AM} and Z_{AM} is non-rotating with respect to the Earth Coordinate System with X_{AM} along the X_E, Y_{AM} along Y_E, and Z_{AM} along Z_E. The origin of the air mass coordinates translates with the average velocity of the wind and coincides with the center of gravity of the aircraft at a particular instant.

The equations derived in this chapter were writted in horizontal and vertical component form; these are written with subscripts "h" and "v" respectively. Horizontal components represent angles in the horizontal air mass plane (X_{AM} - Y_{AM} plane). Vertical components represent angles in the X_{AM} - Z_{AM} plane.

The equations of the fire control problem may be written in component form with respect to various other planes. A convenient approach may be to consider them as components in the lead plane or prediction plane. It was considered desirable in this thesis to write the equations in the horizontal and vertical planes because:

1. The motion of the target was restricted in this thesis to one horizontal plane, although no restrictions were made of target maneuvers in this plane.
2. It may be desired to set up the Attack Simulator either on the ground or to compute with respect to a stabilized platform in the airplane. The horizontal and vertical planes in either case are the most natural representation of the attack problem.

Quantities to be fed back to the Attack Simulator as measurements of interceptor orientation and movement are measured in terms of aircraft coordinates. The origin of the Aircraft Coordinate System is at the center of gravity of the interceptor; Y_A is normal to the plane of symmetry positive along the right wing, X_A is parellel to the projection of the velocity vector on the plane of symmetry in trimmed flight, and Z_A forms a right-hand system. In this thesis, subscripts "e" and "d" represent elevation and deflection components in the Aircraft Coordinate System. Deflection components in aircraft coordinates represent angles in the X_A - Y_A plane. Elevation components represent angles in the X_A - Z_A plane.

Tables A-1 and A-2 of Appendix A give conversions between the Aircraft Coordinate System and the Air Mass Coordinate System using the relating angles H, E, and ϕ in one case and ψ, B, and θ in the other. These angles are defined in Appendix A. Equations (A-1) through (A-8) give relations among these sets of angles.

Quantities may be computed in their natural form as components in radar coordinates or computer coordinates. A discussion of these coordinate systems is given in Appendix B. Elevation and deflection components in radar or computer coordinates are not identical with these components in aircraft coordinates. It is shown in Appendix B

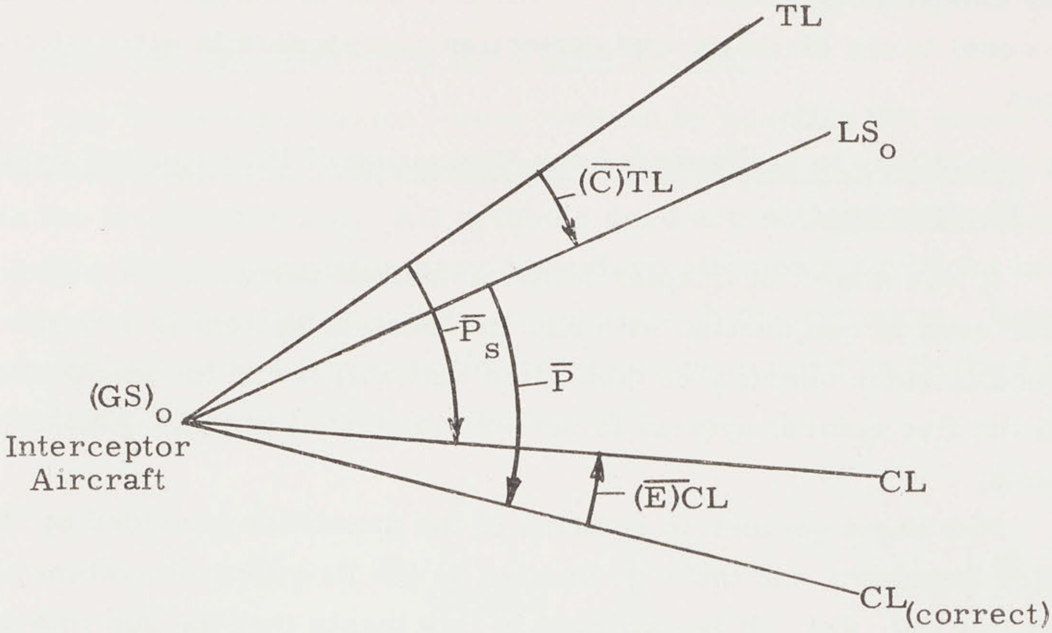

Angles are represented as vector quantities since in general they exist in three-dimensional space.

$\overline{P}$	=	True Prediction Angle (as defined by Attack Simulator)
$\overline{P}_s$	=	Computed Prediction Angle of Fire Control System
$(CL)_{(corr)}$	=	Correct Controlled Line as defined by Attack Simulator
CL	=	Existing Controlled line
$(\overline{C})TL$	=	Tracking Line correction
$(\overline{E})CL$	=	Controlled Line Error

Fig. 6-1 Geometrical relationship between the interceptor aircraft and target.

that these coordinate systems may be related by suitable triginometric functions. It is shown, furthermore, that in the normal attack problem the errors involved are small in assuming elevation and deflections components measured in terms of radar or computer coordinates are equal to the elevation and deflection components in aircraft coordinates.

6.2 Quantities to be Recorded for Evaluation of Fire Control System Performance

It was shown in Chapter 5 that a desired output of the Attack Simulator used in conjunction with any fire control system is a continuous record of some quantity or quantities that will serve to indicate how well the fire control system is performing under various attack conditions.

The basic geometric relation of the quantities provided by the Attack Simulator and those generated by the fire control system are shown in Fig. 6-1. It is assumed in this thesis that the gun line and controlled line of the interceptor are identical.

Prediction error is defined as the difference between the correct prediction angle and the generated prediction angle:
$\overline{(E)P} = \overline{P}_{(corr)} - \overline{P}_s$. A continuous record of the time variation of prediction error would serve as an indication of the dynamic errors of the fire control system.

Controlled line error is defined as the angle between the correct controlled line and the generated controlled line:
$\overline{E}(CL) = \overline{A}_{(CL_{(corr)} - CL)}$. It is apparent that an accurate determination of the time variation of controlled line error would also serve as an indication of the dynamic characteristics of the fire control system. The accurate determination of this quantity depends on:

1. The accuracy with which the existing controlled line orientation can be measured.
2. The accuracy of the Attack Simulator in computing the orientation of the correct controlled line based on defined target motion, measured interceptor motion, and computed ballistic effects.

It was shown in Appendix E that it is possible to correlate controlled line error, range, target area, and a statistical representation of inaccuracies to define whether or not projectiles fired at any particular instant during the attack run will hit or miss the target.

6.3 Equations for Simulating the Attack Problem

The following equations were written by adapting the equations given in Appendix C to the operations required of a system that simulates the attack problem. All symbols used are defined in Appendix C.

The Attack Simulator provides information on a fictitious target moving at a known speed and direction through the air mass. Hence the target speed and target angle may be programmed as desired in accordance with the following equations:

$$V_T = V_{T(\text{initial})} + \int_0^t \dot{V}_T \, dt \qquad (6.1)$$

$$(A_{T_o})_h = \left[(A_{T_o})_h \right]_{(\text{initial})} + \int_0^t \left[(\dot{A}_{V_T})_h - (W_{(LS)_o}) \right] dt \qquad (6.2)$$

In these equations the initial values of target speed and target angles are fixed by the initial conditions of the attack problem; $\dot{V}_T$ and $(\dot{A}_{V_T})_h$ are programmed maneuvers of the target. $\left[W_{(LS)_o} \right]_h$ is computed by the Attack Simulator from:

$$\left[W_{(LS)_o} \right]_h = \frac{1}{R_o \cos D_{(LS)_o}} \left[V_T \sin (A_{T_o})_h - V_{GS} \sin \left[L_h - J_h - (\alpha_C L)_h \right] \right] \qquad (6.3)$$

For a target that flies a straight flight path at constant speed through the air mass, which is the normal flight path required in flight evaluation tests of fire control systems, the equations of target angle and target speed reduce to:

$$V_T = V_{T(\text{initial})} \tag{6.4}$$

$$\left[A_{T_o}\right]_h = \left[A_{T_o}\right]_{h\,(\text{initial})} - \int_0^t \left(W_{(LS)_o}\right)_h \, dt \tag{6.5}$$

The only factors considered in this thesis to be components of prediction angle are lead angle, velocity jump, and gravity drop. Factors that led to this assumption are discussed in Appendix D. The correct lead angle may be computed by the Attack Simulator on the basis of the geometry of the attack problem.

$$(L)_v = \frac{V_T\, t_f}{R_F} \cos\left(A_{T_o}\right)_h \sin D_{(LS)_o} \tag{6.6}$$

$$(L)_h = \frac{V_T\, t_f}{R_F} \; \frac{\sin\left(A_{T_o}\right)_h}{\cos\left(L_v + D_{(LS)_o}\right)} \tag{6.7}$$

Present range to the target is given by:

$$R_o = \left[R_o\right]_{(\text{initial})} + \int_0^t \dot{R}_o \, dt \tag{6.8}$$

$$\dot{R}_o = V_T \cos\left(A_{T_o}\right)_h \cos D_{(LS)_o} - V_{GS} \cos\left[L_h - J_h - (\alpha_{CL})_h\right] \cos\left[L_v + C - J_v - (\alpha_{CL})_v\right] \tag{6.9}$$

The relative bearing to the target is the angle that the line of sight makes with the controlled line. It can be seen from Fig. 6.2 that this angle in component form is as follows:

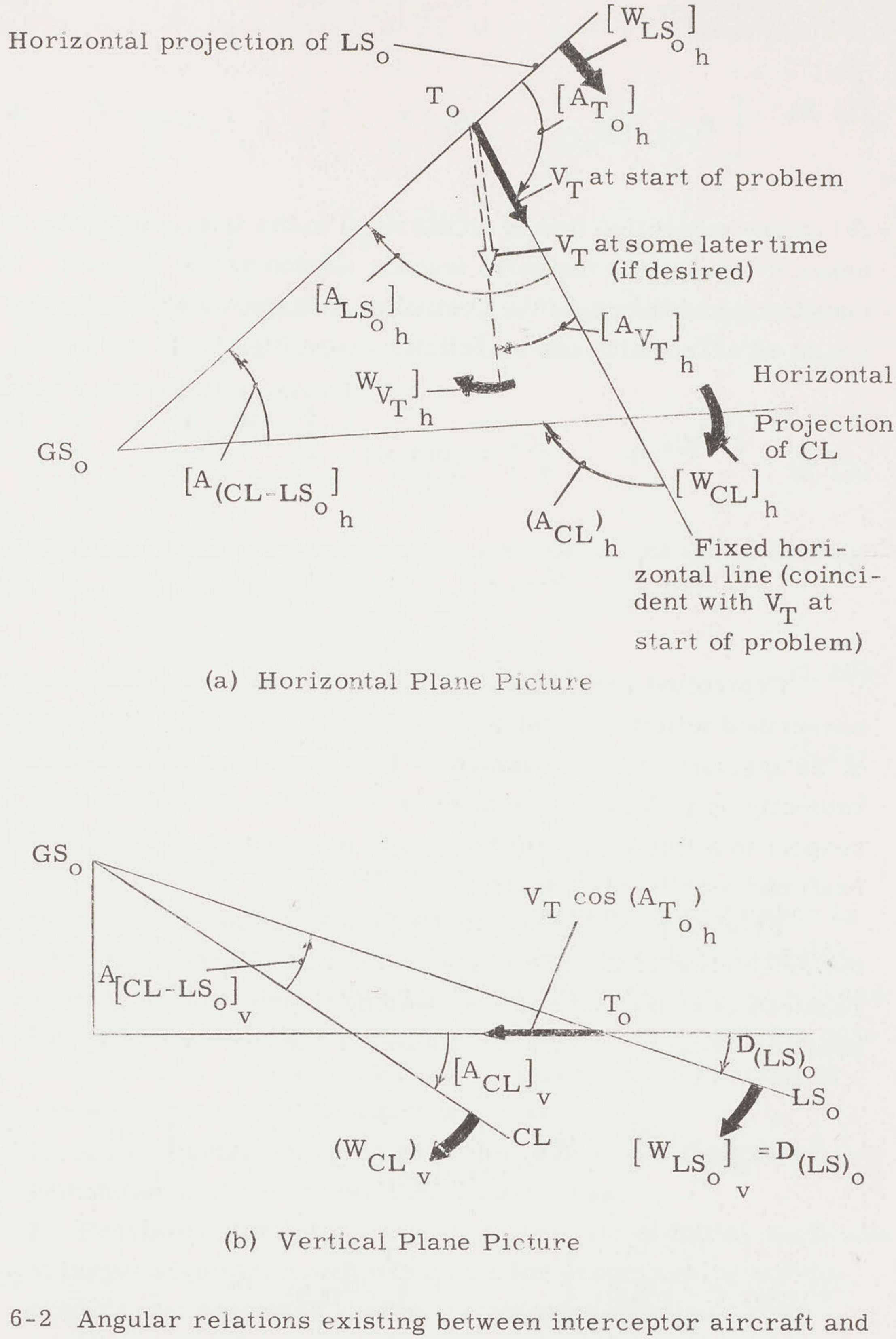

(a) Horizontal Plane Picture

(b) Vertical Plane Picture

Fig. 6-2 Angular relations existing between interceptor aircraft and target.

$$\left[A_{(CL-LS_o)} \right]_h = \left[A_{CL} \right]_h - (A_{LS_o})_h \qquad (6.10)$$

$$\left[A_{(CL-LS_o)} \right]_v = (A_{CL})_v - D_{(LS)_o} \qquad (6.11)$$

The controlled line is a line fixed in the interceptor aircraft, hence it moves with the same angular motion as the aircraft. The components of the angle the controlled line makes with a fixed horizontal reference line are as follows: (see Fig. 6.2)

$$\left[A_{CL} \right]_h = (A_{CL})_{h\,(initial)} + \int_0^t (W_{CL})_h \, dt \qquad (6.12)$$

$$\left[A_{CL} \right]_v = (A_{CL})_{v\,(initial)} + \int_0^t (W_{CL})_v \, dt \qquad (6.13)$$

Controlled line angle is a measurable quantity consisting of the prescribed initial orientation of the aircraft in space and the integral of its angular rate of movement. This angle may be measured conveniently by picking off the angular orientation of the aircraft with respect to a line in a platform that is mounted on gimbals in the aircraft and stabilized in space.

From Fig. 6.2, the following equations are written to represent the orientation of the line of sight in space. These computations are required in order that relative bearing information be continuously available from the Attack Simulator for the fire control system:

$$\left[A_{(LS)_o} \right]_h = 180^o - \left[(A_{T_o})_h \right]_{(initial)} + \int_0^t \left[W_{(LS)_o} \right]_h \, dt \qquad (6.14)$$

$$D_{(LS)_o} = \left[D_{(LS)_o} \right]_{(initial)} + \int_0^t \dot{D}_{(LS)_o} \, dt \qquad (6.15)$$

Alternate expressions for relative bearing may be written as follows from Fig. 6.1:

$$\overline{A}_{(CL-LS_o)} = -\left[\overline{P} + \overline{E}(CL)\right] \tag{6.17}$$

$$\overline{A}_{(CL-LS_o)} = -\left[\overline{P}_s - \overline{(C)}TL\right] \tag{6.18}$$

Controlled line error is measured as the angle between the correct controlled line and the generated controlled line. The correct controlled line angular velocity is:

$$\overline{W}_{CL\ (correct)} = \overline{W}_{(LS)_o} + \dot{\overline{P}} \tag{6.19}$$

The Attack Simulator may measure the controlled line error in component form as follows:

$$\left[(E)CL\right]_v = (P_s)_v - \left[(C)TL\right]_v - P_v \tag{6.20}$$

$$\left[(E)CL\right]_h = (P_s)_h - \left[(C)TL\right]_h - P_h \tag{6.21}$$

6.4 Functional Diagram of the Attack Simulator

An ideal Attack Simulator would be a system located either in the interceptor aircraft or at some remote station which is capable of setting up the attack problem and solving the set of equations listed in section 6.3 with sufficient accuracy to define continuously the correct controlled line orientation in space. Incorporated as integral components of this Attack Simulator would be:

1. All the instrumentation required to measure the interceptor orientation and motion through the air mass.
2. Provisions for setting up any desired set of initial conditions at target acquisition and provisions for programming and desired target speed and course through the air mass.
3. Means for sending the required fictitious target information

to the fire control system to activate the system exactly as it would be activated by a real target.

4. Computing mechanisms to solve the equations of section 6.3. This would require means of solving the ballistic components of prediction angle discussed in Appendix D.

The inputs and outputs of the Attack Simulator are shown in Fig. 6.3. Here the input and output quantities are shown in the component form in which they normally would be measured directly.

Fig. 6.4 is a breakdown of the Attack Simulator into computing components. The equations defining the function of each component in Fig. 6.4 are listed in Table 6.1. The operations of the resolvers are given in Tables A-1 and A-2.

6.5 Results

Upon critical examination of Fig. 6.4 and the computing operations of each component, it is apparent that to simulate the attack problem in its complete form would require a highly intricate and complex system. The design problem involves:

1. The solution of many simultaneous equations that are completely inter-related. Three integrations are involved. In order for the Attack Simulator to provide accurate information on the dynamics of the fire control system, it is necessary that the dynamics of the Attack Simulator itself be reduced to a minimum.
2. The disadvantage of many triginometric operations. These operations may be reduced by small angle approximations of lead and prediction angles, although this approximation may be poor if it is desired to simulate an attack from the beam or forward of the beam on a supersonic target.
3. Three transformations of quantities between the Air Mass and Aircraft Coordinate Systems are required. The transformation from one coordinate system to the other may be simplified by establishing a stable platform in the interceptor utilizing a base motion isolation system.
4. The measurement of the angle of attack of the controlled line. This can be measured either directly with a vane or Prandtl tube,

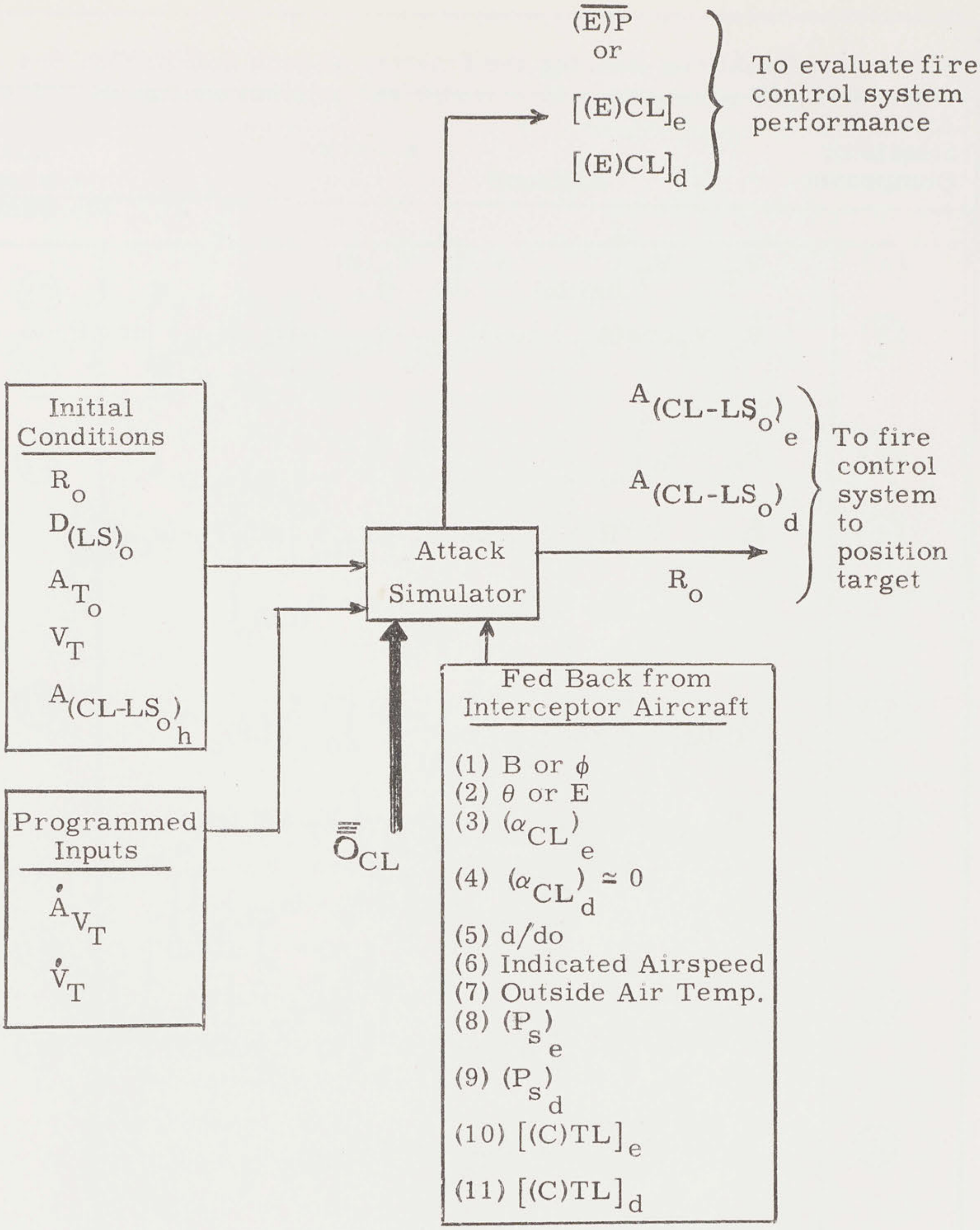

Fig. 6-3 Inputs and outputs of the Attack Simulator.

Table 6-1 Equations defining the function of each unit in Fig. 6-4.

Attack Simulator Component	Equation
(1)	$V_T = V_T\Big]_{initial} + \int_0^t \dot{V}_T \, dt$
(2)	$\dot{R}_o = V_T \cos(A_{T_o})_h \cos D_{(LS)_o} - V_{GS} \cos\left[P_h - (\alpha_{CL})_h\right] \cos\left[P_v - (\alpha_{CL})_v\right]$
(3)	$R_o = R_o\Big]_{initial} + \int_0^t \dot{R}_o \, dt$
(4)	$\dot{D}_{(LS)_o} = 1/R_o \left\{ V_{GS} \cos\left[P_h - (\alpha_{CL})_h\right] \sin\left[P_v - (\alpha_{CL})_v\right] - V_T \cos(A_{T_o})_h \sin D_{(LS)_o} \right\}$
(5)	$D_{(LS)_o} = \left[D_{(LS)_o}\right]_{initial} + \int_0^t \dot{D}_{(LS)_o} \, dt$
(6)	$\left[W_{(LS)_o}\right]_h = \frac{1}{R_o \cos D_{(LS)_o}} \left\{ V_T \sin(A_{T_o})_h - V_{GS} \sin\left[(P)_h - (\alpha_{CL})_h\right] \right\}$
(7)	$\left[A_{T_o}\right]_h = \left[A_{T_o}\right]_{h\ initial} + \int_0^t \left\{ (\dot{A}_{V_T})_h - \left[W_{(LS)_o}\right]_h \right\} dt$
(8)	$L_v = \frac{V_T t_f}{R_F} \cos(A_{T_o})_h \sin D_{(LS)_o}$
(9)	$L_h = \frac{V_T t_f}{R_F} \frac{\sin(A_{T_o})_h}{\cos(L_v + D_{(LS)_o})}$

Table 6-1 Equations defining the function of each unit in Fig. 6-4 (cont.)

Attack Simulator Component	Equation
(10)	$P_v = L_v - J_v + C$
(11)	$P_h = L_h - J_h$
(12)	$A_{(CL-LS_o)_h} = \left[A_{(CL-LS_o)_h}\right]_{initial} + \int_0^t (W_{CL})_h - (W_{LS})_h \, dt$
(13)	$A_{(CL-LS_o)_v} = \left[(A_{CL})_v\right]_{initial} - \left[D_{LS_o}\right]_{initial} + \int_0^t W_{(CL)_v} - D_{LS_o} \, dt$
(14)	$\left[(E)CL\right]_e = (P_s)_e - \left[(C)TL\right]_e - P_e$
(15)	$\left[(E)CL\right]_d = (P_s)_d - \left[(C)TL\right]_d - P_d$

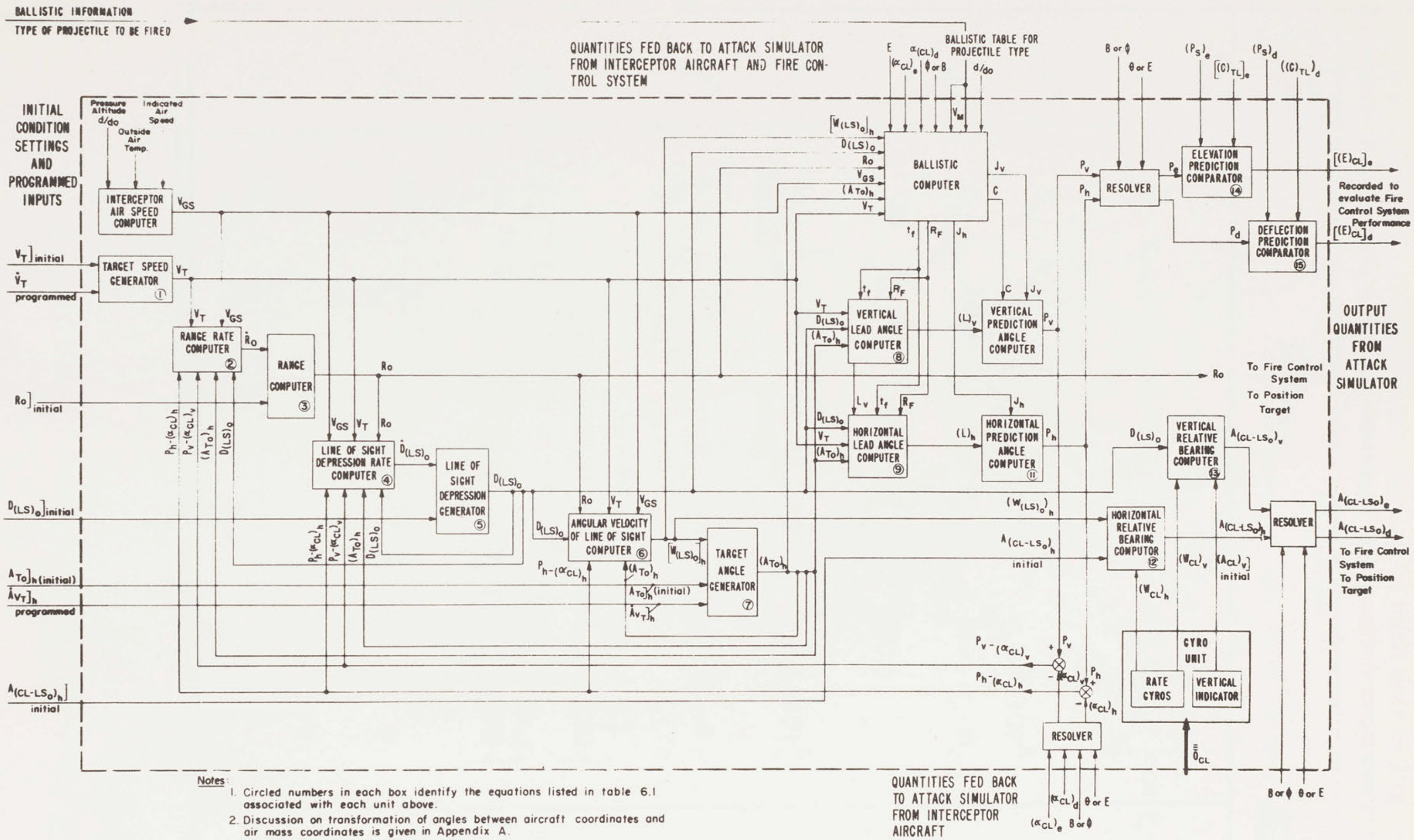

Notes:

1. Circled numbers in each box identify the equations listed in table 6.1 associated with each unit above.
2. Discussion on transformation of angles between aircraft coordinates and air mass coordinates is given in Appendix A.
3. Discussion of ballistic computations is given in Appendix D.
4. Factors involved in determining V_{GS} from indicated air speed not undertaken in this thesis.

FIG. 6.4: **FUNCTIONAL DIAGRAM OF ATTACK SIMULATOR**

or indirectly by taking into account normal accelerations and dynamic pressure. The measurement of angle or attack by present techniques leaves much to be desired in accuracy.

5. A ballistic computer is needed in order to accurately compute future range, time of flight, and gravity drop. The determination of these ballistic properties for a simulated attack, if performed with a high degree of precision, would require a complex computer. The design of a ballistic computer is a science within itself.

6. It is entirely possible to build a mathematical computing machine to solve simultaneously the equations of the form given in Table 6.1. This form of the Attack Simulator may be located at some convenient ground station to set up attack problems for airborne interceptors. The simulator can in this case compute the correct controlled line orientation with an order of accuracy greater than the fire control system since the simulator is unrestricted with respect to size and weight. The initial expense of such a machine would be great; but it might conceivably pay for itself intself just as the modern high-speed mathematical computers pay for themselves because of the speed and accuracy with which they are capable of arriving at solutions of difficult problems.

Transfer of information between the interceptor aircraft in the air and the Attack Simulator on the ground may be accomplished by:

a) Target information telemetered to the interceptor aircraft to activate the fire control system.

b) Measurements of interceptor motion and fire control system output quantities telemetered from the aircraft to the ground.

6.6 Conclusions

The following conclusions were arrived at after a careful consideration of the design factors:

1. If all facets of the attack problem are to be included, then it was concluded that an Attack Simulator with an order of accuracy

greater than the fire control system must inevitably be a ground installation due to the space and weight requirements of a complete system of the form of Fig. 6.4.

2. It was concluded, however, that the Attack Simulator would most effectively take the form of an airborne installation in the interceptor aircraft. In order for the interceptor to work with a ground Attack Simulator, it would be necessary that all evaluation flights be conducted in the vicinity of the ground installation. For fire control systems under development in laboratories at a distant location, additional problems arise in connection with the transportation of maintenance equipment and personnel. It may mean long flights to and from the general vicinity of the Attack Simulator installation for aircraft based within flying range. The aircraft and the ground Attack Simulator would each require a two-way telemetering system. There is a distinct advantage in ease of operation and maximum utilization of flight time if the Attack Simulator is installed in the aircraft with the fire control system. Coordinate transformations are simplified for airborne installations; orientation of the aircraft is transmitted physically to the Attack Simulator. The simulator may be located in close proximity with the fire control system and much of the transfer of information between the two systems can be direct.

3. It was concluded that the incorporation of a separate ballistic computer in the Attack Simulator is unwarranted. If for any reason it should be desired to include ballistic effects in the attack problem (see paragraph 4 following), it is much more practical to accept the ballistic quantities from the fire control system. These quantities are not available in component form in many fire control systems.

Fig. 6.5 shows the inputs and outputs of an Attack that does not incorporate a ballistic computer.

4. It was concluded that the inclusion of ballistic effect in the attack problem itself is not only unnecessary but also undesirable. This conclusion led to an investigation of the kinematic

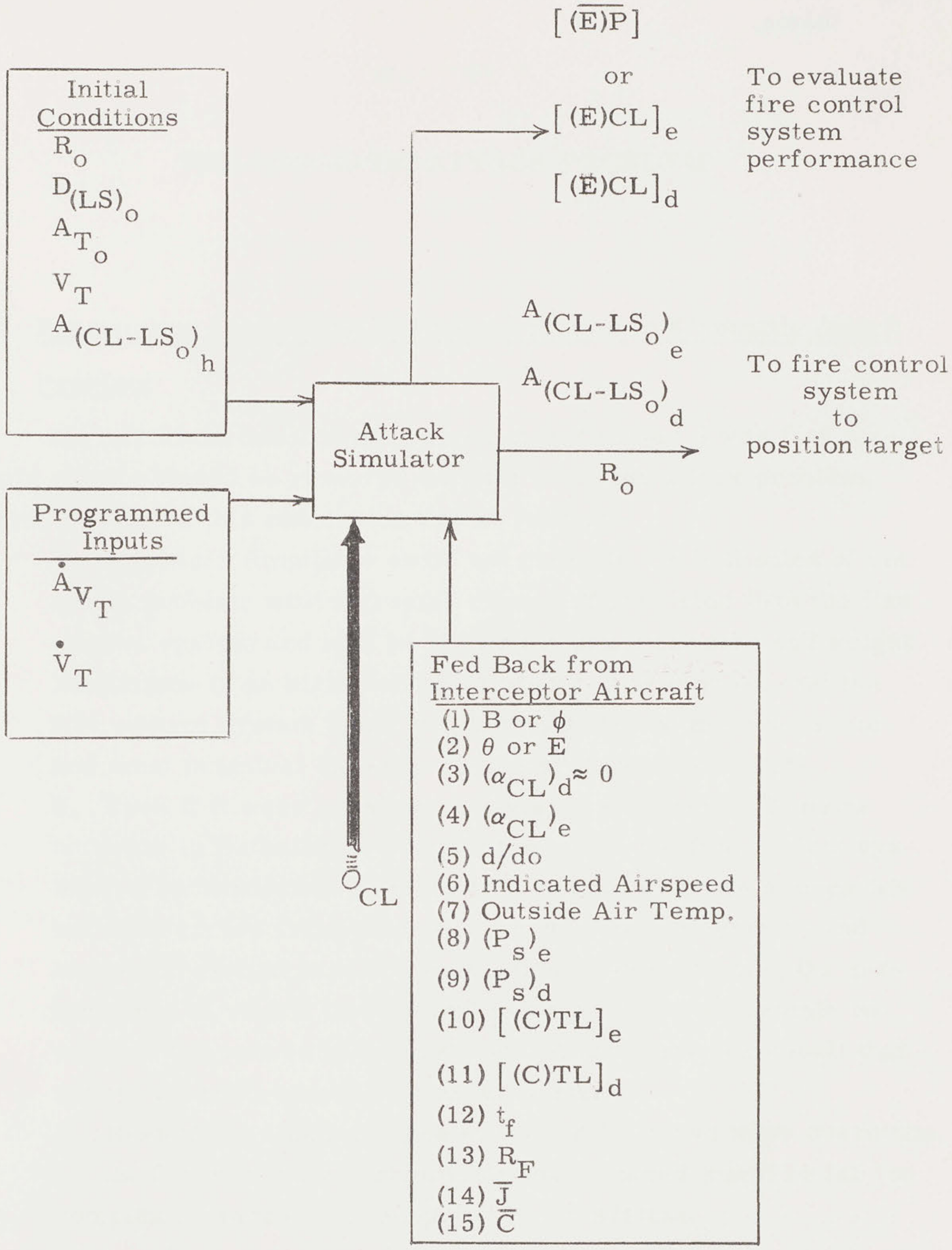

Fig. 6-5 Inputs and outputs of the Attack Simulator that does not incorporate a separate ballistic computer

attack problem. Factors leading to this conclusion and the results of this conclusion are the subject of Chapter 7 of this thesis.

CHAPTER 7

THE KINEMATIC ATTACK PROBLEM

7.1 Reasons for Restricting Evaluation System to Kinematic Attack Problem

An important conclusion arrived at in Chapter 6 was that ballistic effects should be removed entirely from the attack problem. Facts that led to this conclusion are as follows:

1. An Attack Simulator could not compute the ballistics of the attack problem with a greater degree of precision than the fire control system and still be within the practical size and weight limitations of an airborne installation. It is obvious that the fire control system itself will incorporate the most accurate and most practical ballistic computer developed to date.
2. Even if it were possible to devise a system that is more accurate in its ballistic computations than the fire control system, it is impossible in many fire control systems to separate ballistic errors from other errors such as the dynamic and kinematic errors in lead computations. In evaluating the performance of such a fire control system, it is not possible to pinpoint the source of errors even though it may be known that errors do exist somewhere in the system.
3. Even if the disadvantages of (1) and (2) above were overcome, it was shown that the instrumentation required would be far too complex to warrant its inclusion in the system.

7.2 Comparison of the Complete Attack Problem and the Kinematic Attack Problem

The components of predication angle dependent on ballistic effects are:

1. Lead angle: dependent on time of flight and future range.
2. Velocity jump: dependent on projectile initial velocity and gun station orientation with respect to the gun station velocity vector.
3. Gravity drop: dependent on time of flight and air density.

The geometry of the attack problem may be greatly simplified by assuming the trajectory of the projectile is a straight line. Furthermore, the complexity of the problem is reduced if it is assumed the projectile travels at a constant velocity and in the direc- in space the guns are aimed.

If the Attack Simulator were designed to set up this simplified attack problem, the ballistic computer of the fire control system undergoing evaluation tests must be modified such as to make:

$$\bar{J} = 0$$
$$\bar{C} = 0$$
$$(V_{p_o})t_f = R_F$$

The output of the fire control system prediction computer would in this case be $\bar{L}_s$, the computation of which is based on a fixed projectile velocity V_{p_o}.

The space path of the interceptor aircraft in flying a lead pursuit course based on the kinematic problem would be somewhat different from the space path flown in the true pursuit attack. This variation in space path is not important in the determination of dynamic response characteristics of the fire control system. It is recommended that an investigation be undertaken to determine the variation in space paths of an interceptor flying each type of attack when the initial conditions of the attack problem are identical.

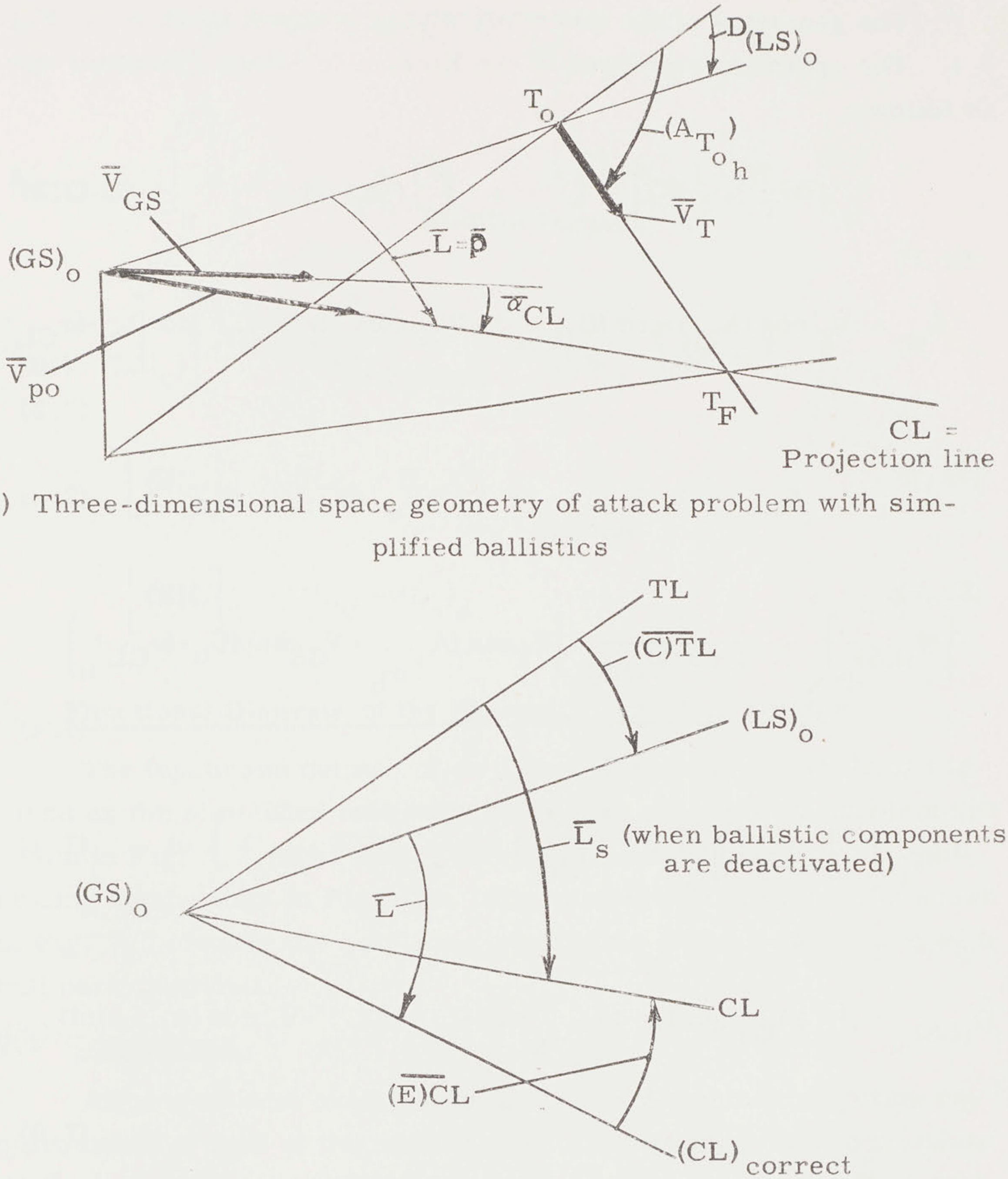

(a) Three-dimensional space geometry of attack problem with simplified ballistics

(b) Comparison of quantities generated by Attack Simulator and those generated by Fire Control System

Fig. 7-1 Geometry of the Kinematic Attack Problem

7.3 Operating Equations of the Kinematic Attack Simulator

The geometry of the kinematic attack problem is shown in Fig. 7.1. The operating equations of the Kinematic Attack Simulator are as follows:

$$V_T = \left[V_T\right]_{initial} + \int_0^t \dot{V}_T \, dt \tag{7.1}$$

$$\dot{R}_o = V_T \cos(A_{T_o})_h \cos(D_{(LS)_o}) - V_{GS} \cos\left[L_h - (\alpha_{CL})_h\right] \cos\left[L_v - (\alpha_{CL})_v\right] \tag{7.2}$$

$$R_o = \left[R_o\right]_{initial} + \int_0^t \dot{R}_o \, dt \tag{7.3}$$

$$\left[W_{(LS)_o}\right]_h = \frac{1}{R_o \cos D_{(LS)_o}} \left[V_T \sin(A_{T_o})_h - V_{GS} \sin(L_h - (\alpha_{CL})_h\right] \tag{7.4}$$

$$(A_{T_o})_h = \left[(A_{T_o})_h\right]_{initial} + \int_0^t \left[(\dot{A}_{V_T})_h - (W_{(LS)_o})_h\right] dt \tag{7.5}$$

$$\dot{D}_{(LS)_o} = \frac{1}{R_o} \left[V_{GS} \cos(L_h - (\alpha_{CL})_h) \sin(L_v - (\alpha_{CL})_v) - V_T \cos(A_{T_o})_h \sin D_{(LS)_o}\right] \tag{7.6}$$

$$D_{(LS)_o} = \left[D_{(LS)_o}\right]_{initial} + \int_0^t \dot{D}_{(LS)_o} \, dt \tag{7.7}$$

$$(L)_v = \frac{V_T}{V_{p_o}} \cos(A_{T_o})_h \sin D_{(LS)_o} \tag{7.8}$$

$$(L)_h = \frac{V_T \sin (A_{T_{o_h}})}{V_{p_o} \cos (L_v + D_{(LS)_o})} \tag{7.9}$$

$$\left[A_{(CL-LS_o)}\right]_h = \left[A_{(CL-LS_o)}\right]_{h(initial)} + \int \left[(W_{CL})_h - (W_{(LS)_o})_h \right] dt \tag{7.10}$$

$$\left[A_{(CL-(LS)_o)}\right]_v = (A_{CL})_{v(initial)} - D_{(LS)_o} + \int (W_{CL})_v \, dt \tag{7.11}$$

$$\left[(E)L\right]_e = (L)_e - (L_s)_e \tag{7.12}$$

$$\left[(E)L\right]_d = (L)_d - (L_s)_d \tag{7.13}$$

7.4 Functional Diagram of the Kinematic Attack Simulator

The inputs and outputs of an Attack Simulator whose design is based on the simplified ballistics of the kinematic attack problem are shown in Fig. 7.2. The Attack Simulator is subdivided into its operating components in Fig. 7.3. The numbers within the units shown in Fig. 7.3 identify the equation given in this chapter associated with that particular unit.

7.5 Conclusions

After a critical examination of Fig. 7.3 and the computing requirements of each of the components, it is apparent that to simulate the kinematic attack problem requires a complex system. It may be seen that three integrations and three coordinate transformations are required. The complexity of the system, however, is greatly reduced from that of the Attack Simulator which simulates a complete attack problem.

Conclusions arrived at were:

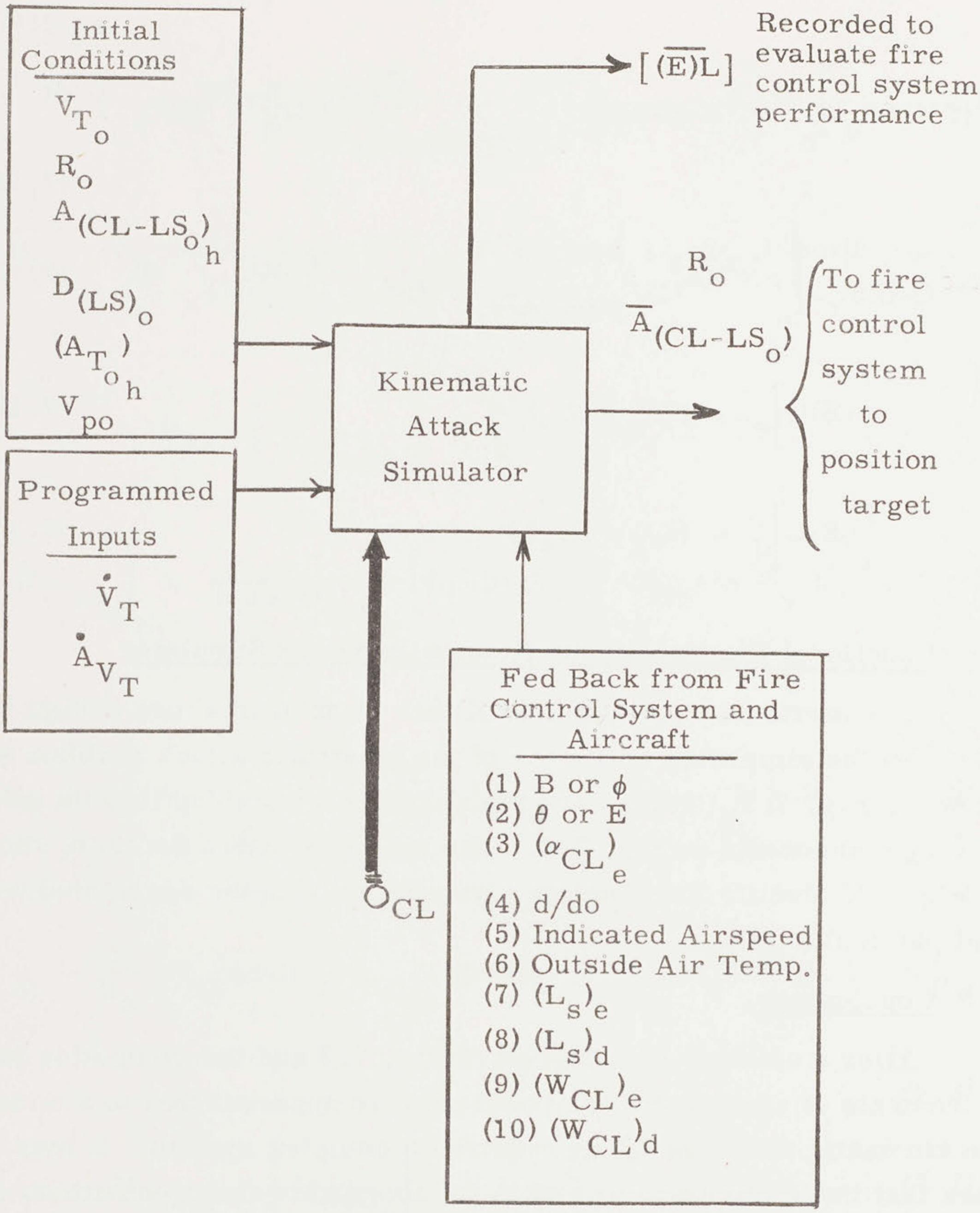

Fig. 7-2 Inputs and outputs of the kinematic attack simulator.

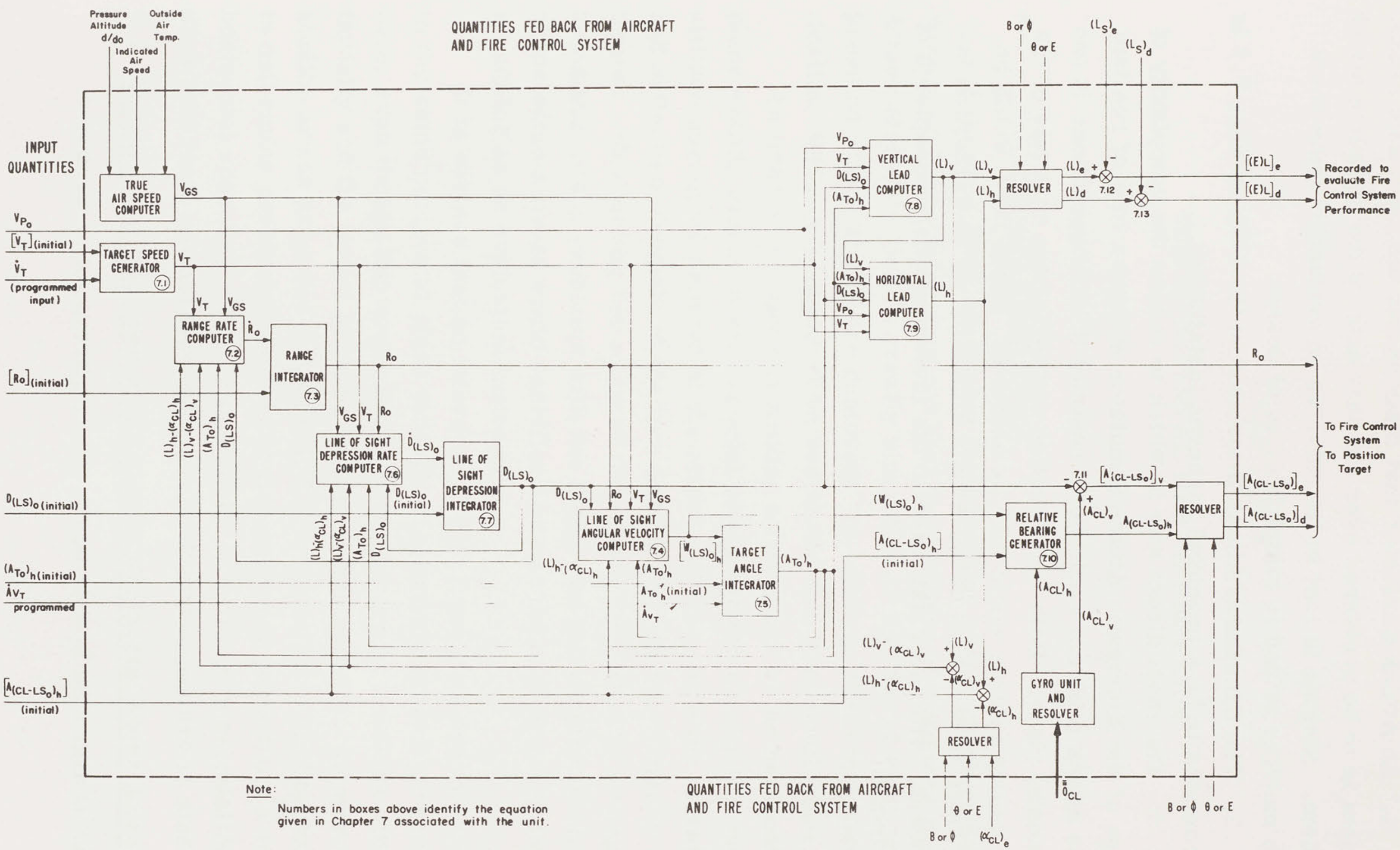

Note:

Numbers in boxes above identify the equation given in Chapter 7 associated with the unit.

FIG. 7.3 **FUNCTIONAL DIAGRAM OF KINEMATIC ATTACK SIMULATOR**

1. An Attack Simulator that instruments the kinematic attack problem is to be preferred over one that sets up the complete attack problem. Nothing is lost in its value as an evaluation instrument while much is gained in simplification of design.

2. The Kinematic Attack Simulator in the form of Fig. 7.3 is too complex to be a practical airborne installation.

3. The most direct way in which to reduce the complexity of design of the Kinematic Attack Simulator without a loss of realism in the attack problem would be to restrict it to computations in one horizontal plane. Both the elevation and deflection channels of the fire control system would still be activated, hence little would be sacrificed in the value of the Attack Simulator as an evaluation instrument. This conclusion led to the investigations of Chapter 8 of this thesis.

CHAPTER 8

THE HORIZONTAL PLANE PROBLEM

8.1 The Horizontal Plane Attack

It is seen after examining the equations of the attack problem developed in previous chapters that the problem of designing the Attack Simulator can be greatly simplified if the line of sight depression computations are removed. In order to effect this simplification, the attack run must be restricted to a horizontal plane.

An interceptor aircraft making a firing run in the horizontal plane would, except in very special attack situations, fly in a banked altitude during all or most of the attack. Hence, both the elevation and deflection channels of the fire control system are normally activated. Restricting the scope of the Attack Simulator to setting up kinematic attack problems with the target and interceptor initially at the same altitude would sacrifice little in the usefulness of the simulator as an evaluation instrument.

It is obvious that an interceptor with fixed guns does not remain in the same horizontal plane throughout a kinematic lead pursuit attack, even though the target and interceptor are at the same altitude initially and the target always remains at this altitude. Numerical studies are in progress at the M.I.T. Instrumentation Laboratory to determine precisely how far the interceptor departs from a truly horizontal space path in such an attack. Preliminary calculations show that for a normal lead pursuit attack this departure is small.

8.2 Assumptions Required to Simulate a Horizontal Plane Attack

It is desired to investigate the properties of an attack in the horizontal plane; i.e. $D_{(LS)_o} = 0$.

It is shown in Chapter 7 that in the three-dimensional kinematic attack problem, the geometric relation between the target and interceptor is a function of line of sight depression angle. This angle is as follows:

$$D_{(LS)_o} = \left[D_{(LS)_o}\right]_{(initial)} + \int \frac{1}{R_o} \left\{ V_{GS} \cos\left[L_h - (\alpha_{CL})_h\right] \sin\left[L_v - (\alpha_{CL})_v\right] \right.$$

$$\left. - V_T \cos (A_{T_o})_h \sin D_{(LS)_o} \right\} dt \qquad (8.1)$$

Assuming the interceptor and target are initially at the same altitude, then $\left[D_{(LS)_o}\right]_{(initial)} = 0$. With this restriction, it is seen that $D_{(LS)_o}$ will be zero at all times during the attack run only if:

$$(L)_v = (\alpha_{CL})_v \qquad (8.2)$$

In a truly horizontal attack with no jump or gravity effects on the trajectory, the vertical component of lead angle is zero. As the vertical component of angle of attack changes, the guns will tend to be aimed out of the horizontal plane. To restrict the aiming of the guns to the horizontal plane:

1. Either the fixed-gun interceptor flies a space path that is not in the horizontal plane.
2. Or the guns of the interceptor are movable to the extent that they can always be aimed in the horizontal plane with angle of attack changes.

For purposes of determining simplifications in the design of the Attack Simulator, it was assumed that $D_{(LS)_o} = 0$ throughout the attack run.

8.3 Operating Equations of the Attack Simulator

The equations that must be solved by the Attack Simulator restricted to the two-dimensional horizontal attack problem were written by setting $D_{(LS)_o} = 0$ in the equations of Chapter 7. The resulting equations were as follows:

$$V_T = \Big[V_T\Big]_{(initial)} + \int_0^t \dot{V}_T \, dt \qquad (8.3)$$

$$\dot{R}_o = V_T \cos (A_{T_o})_h - V_{GS} \cos (L_h - (\alpha_{CL})_h) \qquad (8.4)$$

$$R_o = R_o\Big]_{initial} + \int_0^t \dot{R}_o \, dt \qquad (8.5)$$

$$\Big[W_{(LS)_o}\Big]_h = \frac{1}{R_o}\Big[V_T \sin (A_{T_o})_h - V_{GS} \sin (L_h - (\alpha_{CL})_h\Big] \qquad (8.6)$$

$$A_{T_o}\Big]_h = A_{T_o}\Big]_{initial} + \int_0^t \Big[(\dot{A}_{V_T})_h - (W_{(LS)_o})_h\Big] dt \qquad (8.7)$$

$$L_v = (\alpha_{CL})_v \qquad (8.8)$$

$$L_h = \frac{V_T}{V_{p_o}} \; \frac{\sin (A_{T_o})_h}{\cos (\alpha_{CL})_v} \qquad (8.9)$$

$$\Big[A_{(CL-LS_o)}\Big]_h = A_{(CL-LS_o)_h}\Big]_{initial} + \int \Big[(W_{CL})_h - (W_{(LS)_o})_h\Big] dt \qquad (8.10)$$

$$[(E)L]_e = (L)_e - (L_s)_e \qquad (8.11)$$

$$[(E)L]_d = (L)_d - (L_s)_d \qquad (8.12)$$

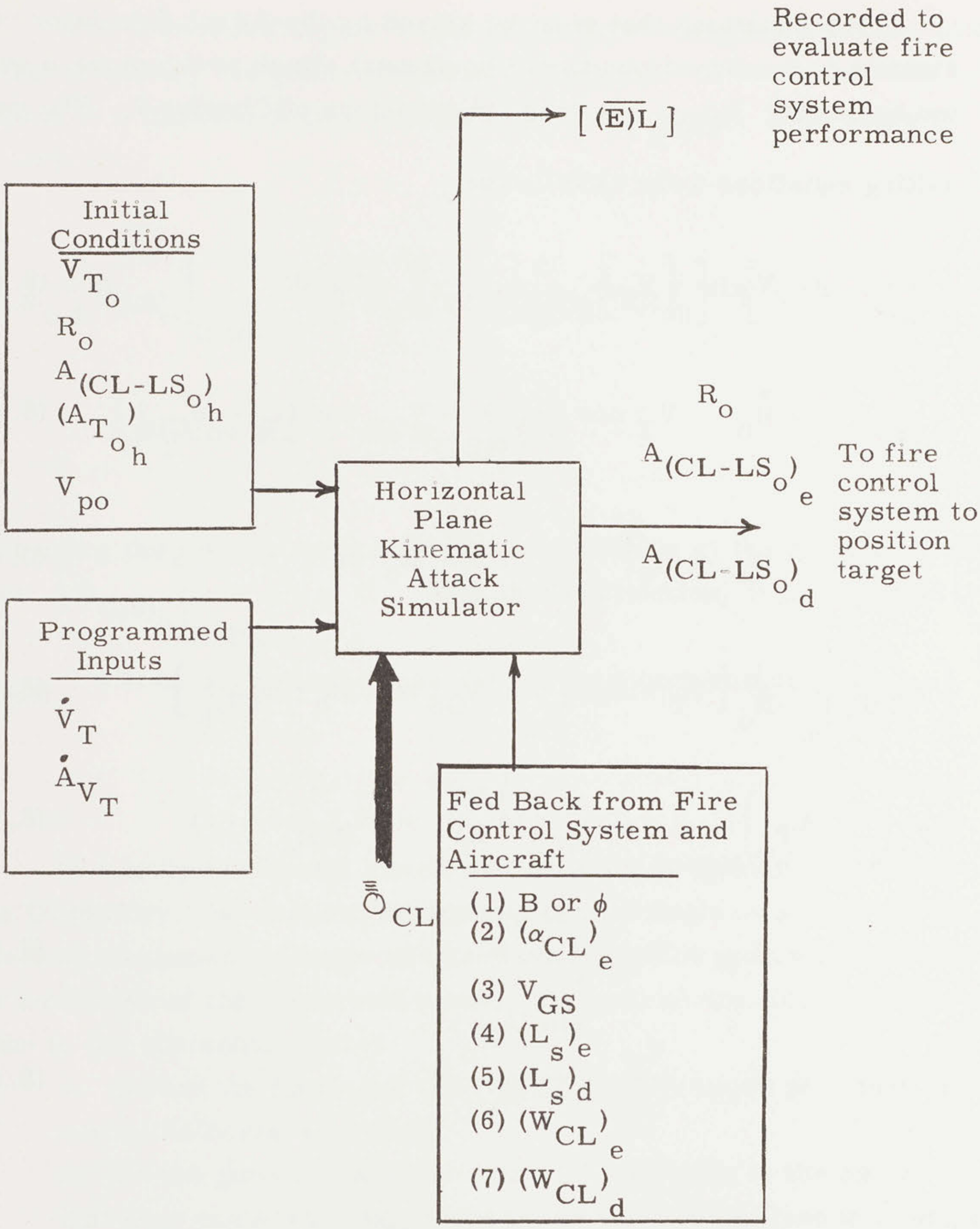

Fig. 8-1 Inputs and outputs of the Kinematic Attack Simulator
Restricted to horizontal plane problem

8.4 Functional Representation of the Attack Simulator Restricted to the Horizontal Kinematic Attack

Input and outputs of the Attack Simulator, under the restrictions of this chapter, are shown in Fig. 8.1. The Attack Simulator is represented functionally in Fig. 8.2. The numbers within the units shown in Fig. 8.2 identify the operational equation of that unit with the equations of this chapter.

8.5 Conclusions

It is seen from an examination of Fig. 8.3 and the computing requirements of each of the components that considerable simplification in the design of the Attack Simulator is possible when compared to the design previously investigated. Three coordinate transformations are required but the number of integrations is reduced to two.

It was concluded that:

1. The advantage is simplification of design for this form of the Attack Simulator is greater than the disadvantage of a restriction on the scope of attack problems it may set up. Nothing is lost in the value of the Attack Simulator as an evaluation instrument since both the elevation and deflection channels of the fire control system are activated.

2. The accuracy of the time variation of lead angle error recorded is poorer than that of Attack Simulators in the form discussed previously due to the assumption that $D_{(LS)_o} = 0$. Before the true value of the form of the Attack Simulator investigated here can be determined, it is necessary that a complete study be undertaken to determine the effect of assuming $D_{(LS)_o} = 0$ on the accuracy with which correct lead angle can be computed. Preliminary calculations of one attack situation indicate that this assumption may be satisfactory, though no numerical information is available at this time.

3. If the errors in lead computation resulting from the assumption that $D_{(LS)_o} = 0$ are negligible, then it was concluded

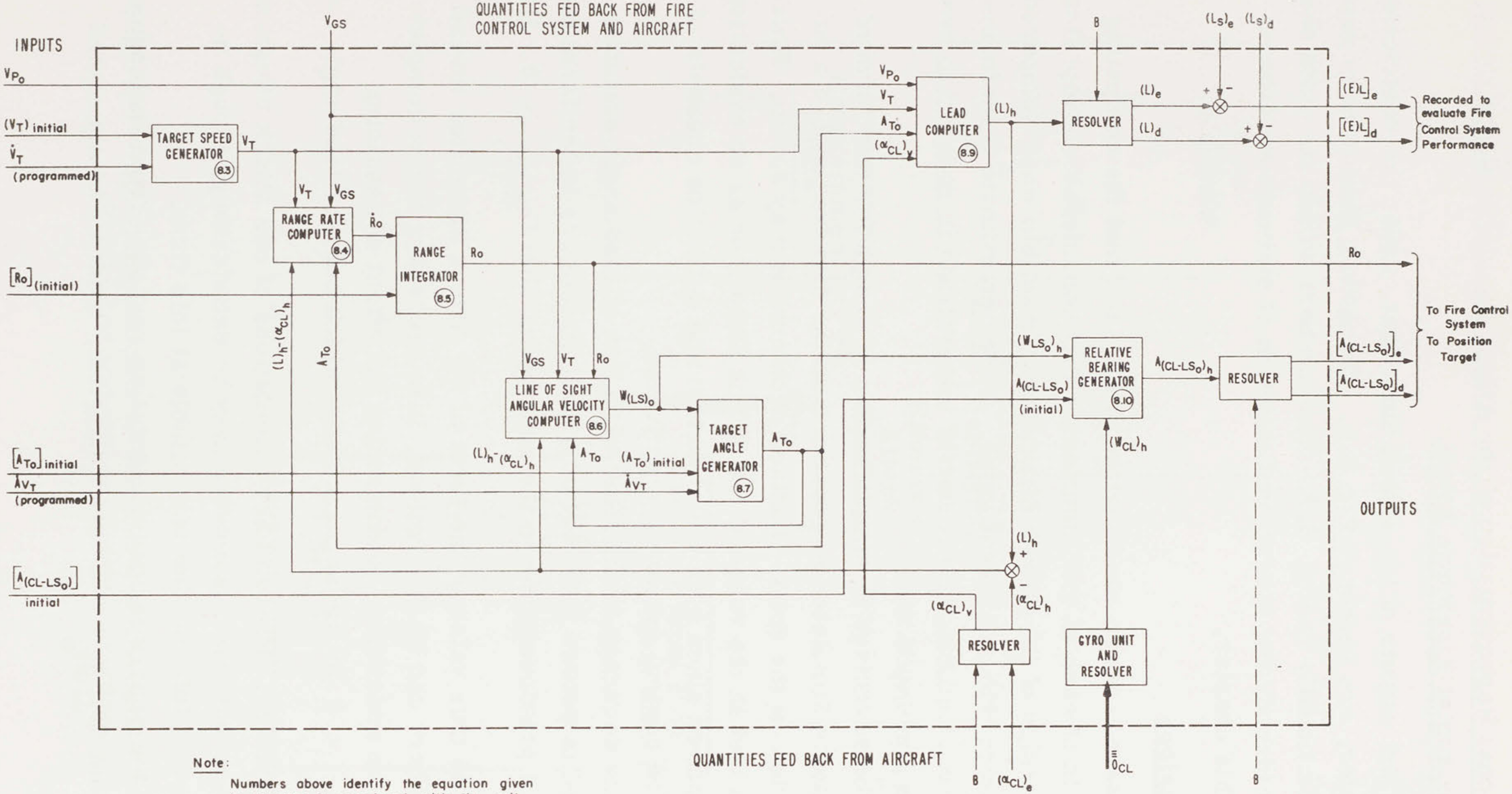

Note:
Numbers above identify the equation given in Chapter 8 associated with the unit.

FIG. 8.2 FUNCTIONAL DIAGRAM OF KINEMATIC ATTACK SIMULATOR RESTRICTED TO HORIZONTAL PLANE ATTACK PROBLEM that the form of the Attack Simulator investigated here would be more practical than any of the forms discussed in previous chapters of this thesis.

4. If it is desired that the Attack Simulator be capable of simulating realistic attack problems, and at the same time provide useful and accurate evaluation information, it was concluded that no further simplifications are possible in the complexity of design without departing from the concept of programming target motion in space.

CHAPTER 9

AIRBORNE ATTACK SIMULATOR DESIGNED PRIMARILY TO ACTIVATE THE FIRE CONTROL SYSTEM

It was concluded from the investigations discussed in previous chapters of this thesis that the complexity of the Attack Simulator System could not be reduced sufficiently for practical airborne installation without departing from the concept of programming the motion of the fictitious target along a particular path in space.

9.1 The Need for a Tracking Simulator

The first consideration in the evaluation of any newly-designed automatic fire control system is primarily a search for the answers to the following questions:

1. Does the system have a sufficient degree of stability throughout its range of operation?
2. Does the system track the target with an acceptable degree of accuracy?
3. If either of the answers to the questions above are negative, within what part of the system does the trouble exist?

The answers to these questions, and to other basic questions, can be given by an Attack Simulator that does little more than activate the tracking system.

9.2 Functional Design of the Tracking Simulator

An Attack Simulator that programs angular velocity of the line of sight could be the cure, in many cases, to the designers' headaches that revolve around the pointers discussed in section 9.1. An Attack Simulator of this type would most effectively take the form of a programmed movement in space of a stabilized platform in the airplane.

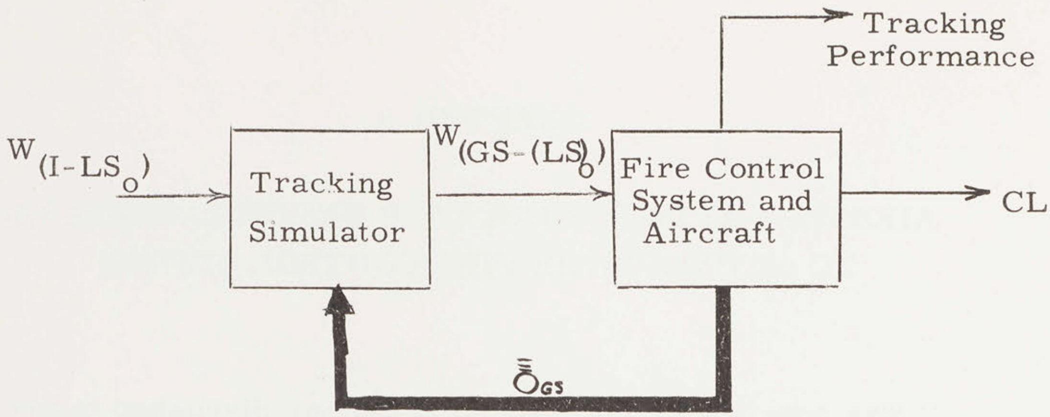

Fig. 9-1 The Tracking Simulator evaluation system

Fig. 9-1 is a functional diagram of an Attack Simulator that involves only the programmed input of the angular velocity of the line of sight to the target. This form of the Attack Simulator is called the Tracking Simulator in this thesis.

9.3 Method of Stabilizing the Platform of the Tracking Simulator

The Tracking Simulator of Fig. 9.1 may consist of the programmed movement of a platform that is stabilized in space from all other inputs except a command signal. A line in the platform of the Tracking Simulator may represent the orientation of the present line of sight to the target. The platform may be mounted on three gimbals as shown in Fig. 9.2. On this platform, three single-degree-of-freedom integrating gyros are mounted with mutually perpendicular axes. A brief discussion of the single-degree-of-freedom integrating gyro is given in Appendix F.

The three gyros mounted on the controlled platform will detect any angular deviations of the platform relative to the inertial space coordinate system. The outputs of the gyros may be used as error signals for three servo systems that orient the stable platform about the three isolation axis in such a way as to null the outputs of the gyros. Thus, the controlled member can be stabilized with respect to inertial reference axes. Consequently, any rotary motion of the aircraft caused by gust disturbances or changes in heading will not affect the inertial orientation of the line of sight defined by the Tracking Simulator.

9.4 Angular Rotation of the Line of Sight

In the Tracking Simulator, it is desired to move the controlled member in inertial space according to a command drive signal. This may be accomplished by using a torque generator and an angular deviation receiver. The torque generator may be mounted on the output axis of the angular deviation receiver to produce a torque proportional to the command drive signal. The output axis of the integrating gyro unit cannot tell the difference between the torque produced by the torque generator and the torque produced by the gyro. Consequently, the unit should act as though it had moved away from the reference axis by an angle proportional to the integral of the torque supplied by the torque generator; and the Tracking Simulator stabilization system servos then would drive the gimbals in accordance with the integral of the command signal. The command signal is proportional to the angular velocity of the line of sight in air mass space.

9.5 Activating the Fire Control System

A line in the platform of the Tracking Simulator represents the orientation of the line of sight to the target. It was shown in section 9.4 that the orientation of this line is space may be moves as desired by a command drive signal. The configuration of the elevation and deflection gimbals of the Tracking Simulator are identical with the configuration of the radar elevation and deflection gimbals, hence the difference in orientation between the fictitious line of sight and the radar tracking line is easily measured; this is the tracking line error.

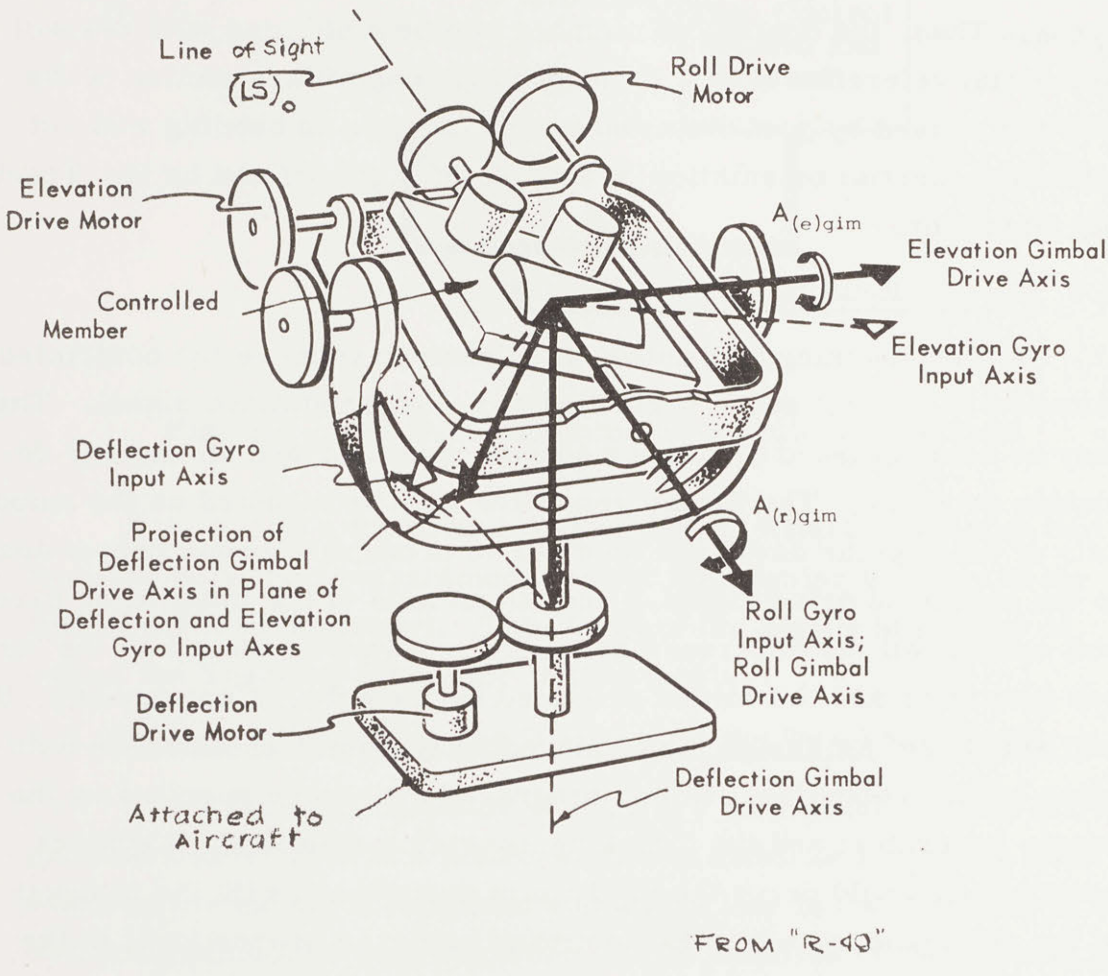

Fig. 9-2 Axis system of the tracking simulator gyro package

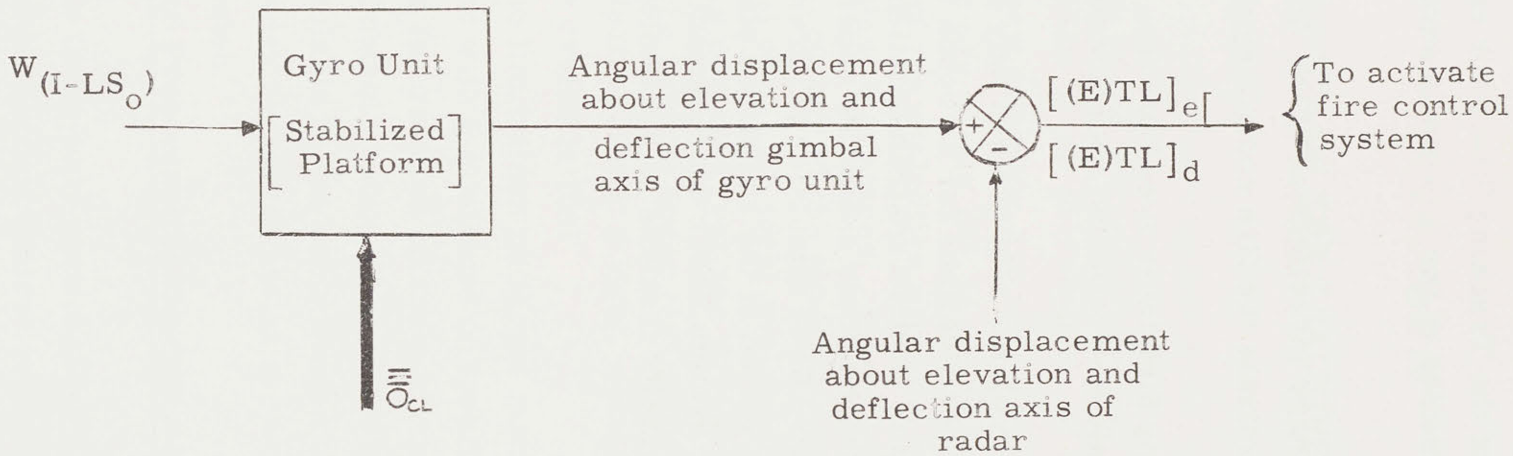

Fig. 9-3 Operation of the Tracking Simulator

The elevation and deflection drive motors of the radar may be activated by a signal proportional to the difference in angular displacement of the gimbals of the Tracking Simulator and those of the radar. A functional representation of the system is shown in Fig. 9.3.

9.6 Conclusions

After a preliminary investigation of the Attack Simulator designed primarily to activate the fire control system, it was concluded that:

1. The Tracking Simulator would provide valuable information on the in-flight dynamic performance characteristics of the fire control system.

2. An Attack Simulator of this form may be built within reasonable size and weight specifications for airborne installation and is within the capabilities of modern instrumentation techniques.

3. A detailed design study should be undertaken of this system as the first phase of an Attack Simulator program. This could be done as a special application of the stabilized platform of the Black Warrior Fire Control System under development at the Instrumentation Laboratory, Massachusetts Institute of Technology, Cambridge, Mass.

CHAPTER 10

REFINEMENTS OF THE TRACKING SIMULATOR

10.1 Requirements of the Evaluation System

In the evaluation of the performance of any new single piece of equipment or any new complete system, whether it be a complete weapons system or any single link in the weapons system chain, the answers required of the evaluation program may be a rough approximation in the earliest test stages. As the system under evaluation is improved, the accuracy of the evaluation procedure must also improve to keep ahead of it. An ideal evaluation system would be one that is as simple as possible, yet one with accuracy of evaluation that increases as the system under test progresses.

It is highly desirable that a light, compact Airborne Attack Simulator be made available that

(1) Places no limitations on target motion.

(2) Performs with a minimum of dynamic effects.

(3) Provides information on the perfromance characteristics of the Fire Control System such that order of magnitude answers are available in the early stages of equipment design and precise answers are available as the equipment under evaluation is perfected.

10.2 Advantages of Precomputing the Space Geometry of the Attack Problem

Certain basic ideas were apparent by looking again at the overall mission desired of the fire control evaluation system.

(1) The easiest way to cut down on the size and complexity of the Attack Simulator would be to decrease to an absolute

minimum the mathematical computations and measurements required.

(2) A fundamental way to reduce the mathematical computations would be to pre-compute and provide programmed solutions for as many of the quantities as possible.

(3) The Fire Control System is designed such as to control the interceptor along a certain space path. Normally the lead pursuit course is that which would be flown by the interceptor in its ideal response to the geometry of the attack problem. The Fire Control System may be built, however, to make available other types of attack runs. These may be:

(a) Pure pursuit.

(b) Snap shooting.

(c) Collision.

For discussion purposes, the lead pursuit course only was investigated here. If the attack problem is set up at:

(a) a given altitude

(b) given initial conditions at target acquisition

(c) prescribed target velocity and course

(d) a certain type airplane with prescribed initial velocity and orientation along the lead pursuit path

(e) a prescribed type of projectile

then the interceptor would fly one ideal path in space in its attack provided no evasive maneuvers were made and gust interference were neglected.

Since the end result of a perfectly designed Fire Control System would be the continuous positioning of the interceptor along this fixed space path for any given problem, deviations from this space path for any non-ideal Fire Control System would show up as errors in the solution when compared to the ideal attack run. Hence, values may be computed and programmed for the movement of the line of sight, present range, and correct prediction angle for each set of initial conditions under which it is desired to evaluate Fire Control System performance. The computation of these values for each attack situation is a tedious iterative process, but the fact that they are computed and provided in advance removes this difficult job from the Attack Simulator.

4. Programmed quantities that essentially depend on interceptor motion and orientation are not precisely correct quantities at any given instant during the attack run if the interceptor has departed from the space path prescribed in the computation of the quantities. From the Attack Simulator point of view, the fictitious target does not move through space precisely as programmed if the interceptor departs from its ideal space path. That is, the $\overline{R}_o$ vector, which is tied at its base to the interceptor and tied at its tip to the target, moves in space dependent on how it is pushed at the base and pulled at the tip. If its motion in space is programmed, then when the base of the vector moves in a manner that is different from the way it ideally would, the tip effectively does not move as prescribed. As a result, a prediction angle that is programmed as correct would not, in general, be the true prediction angle. A programmed "correct" prediction angle would be less accurate the further the interceptor departs from its ideal space path.

5. The acceptance of order of magnitude answers when the base of the $\overline{R}_o$ vector has departed significantly from its ideal position, and the fact that these answers are more correct when the base of this vector is where it should be, may make it unnecessary to feed back information on interceptor motion in order to get usable performance information about the fire control system.

10.3 Functional Design of the Attack Simulator with Programmed Inputs

Programmed inputs based on initial conditions, altitude, desired interceptor path, prescribed target motion, etc. may be computed prior to the flight and the following quantities provided:

1. Angular velocity of the line of sight.
2. Present range.
3. Correct Prediction Angle.

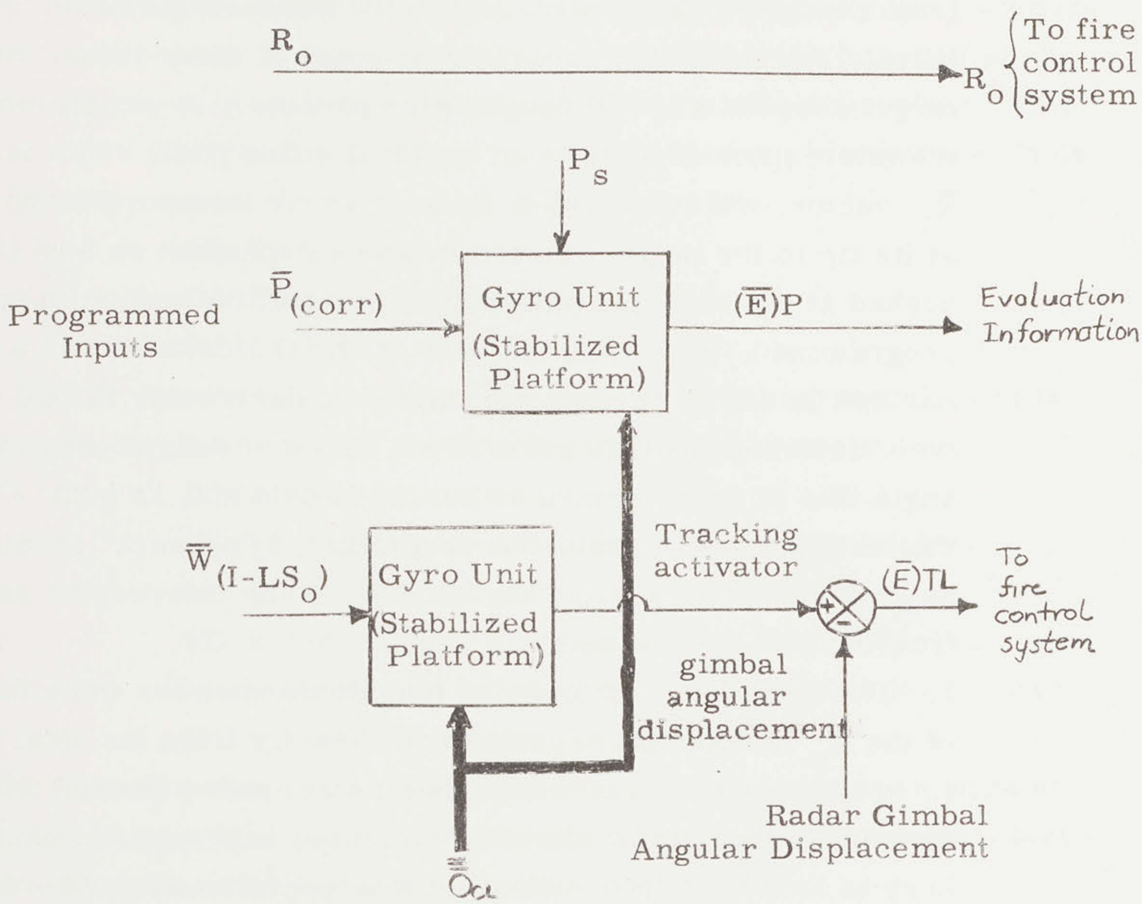

Fig. 10-1 Functional design of airborne Attack Simulator using simultaneously programmed inputs

The functional design of this form of the Attack Simulator is shown in Fig. 10.1.

The programmed angular velocity to this system may be instrumented in the same manner as the system described in Chapter 9. The primary difference here is that the angular velocity of the line of sight to the Tracking Simulator may be any arbitrary input, while that to the system shown in Fig. 10.1 must be precisely computed in advance for a particular attack problem.

10.4 Conclusions

It was concluded that:

1. Before the true value can be established for the Attack Simulator system of the form discussed in this chapter, an investigation should be undertaken in order to determine the accuracy with which the dynamic characteristics of fire control systems can be evaluated under normal flight conditions when the angular velocity of the line of sight, present range, and correct prediction angle are simultaneously programmed for typical lead pursuit attacks under prescribed initial conditions.

2. The possibility of modifying programmed values of range and prediction angle in order to correct them for actual interceptor motion in response to the attack problem should be investigated. This investigation would be of particular value if the studies recommended in (1) above should turn out negative.

3. The next step forward in the design program of an Airborne Attack Simulator system over the system outlined in Chapter 9 would be a system of the general type discussed here utilizing information fed back from the interceptor on the time variation of angle of attack and velocity to modify programmed values of correct range and prediction angle.

APPENDIX A

DEFINITION OF COORDINATE SYSTEMS

When the performance of an interceptor aircraft is to be analyzed, a variety of coordinate systems is required. The interceptor is vectored to the target with information supplied from ground stations, and hence in Earth Coordinates. Once the target is acquired by the interceptor radar, the fire control problem must be solved with respect to a fixed reference space since the gyroscopic elements used in the computer are sensitive to absolute angular velocities.

These angular velocities must be resolved along the gyroscopic input axes or computer axes. Closed-loop tracking systems have computer axes non-rotating with respect to the aircraft, whereas open-chain tracking systems have computer axes fixed with respect to the radar antenna. The computer coordinates are defined more completely in Appendix B.

When the heading of the aircraft is in error, corrections are applied by use of the elevator, rudder, and ailerons, which provide moments about the aircraft body axes. The most convenient aircraft coordinates are those used by the NACA when supplying aerodynamic force and moment data. These Aircraft axes, as well as Earth-Reference axes, Earth-Aircraft axes, Earth Plane of Symmetry axes, and the Air Mass axes are defined as follows:

The Aircraft Coordinate System, X_A, Y_A, Z_A, shown in Fig. A-1, has its origin at the center of gravity of the aircraft with Y_A normal to the plane of symmetry (positive along the right wing), X_A parallel to the projection on the plane of symmetry of the velocity vector in trimmed flight (positive forward), and Z_A forming a right-hand system.

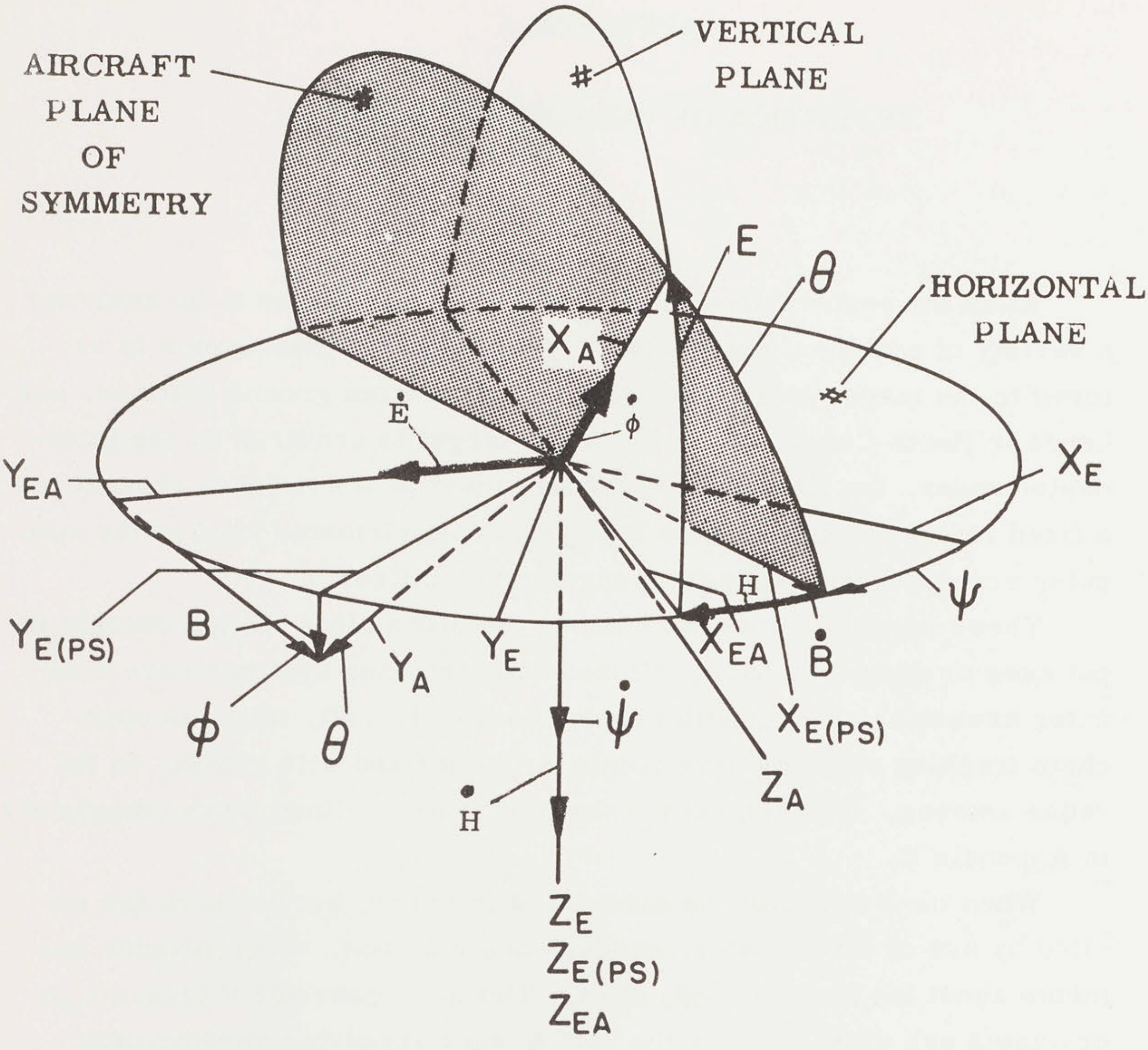

taken from "T-10"
"REFERENCE 2"

Fig. A-1 Relationships among coordinate systems used in an analysis of interceptor aircraft.

The velocity vector is a measure of the speed and direction of the aircraft with respect to the air mass.

The Earth Coordinate System, X_E, Y_E, Z_E has its origin at the aircraft center of gravity, with Z_E along the vertical (positive downward), X_E in a convenient fixed geographic heading, and Y_E forming a right-hand system.

The Earth-Aircraft Coordinate System, X_{EA}, Y_{EA}, Z_{EA}, has its origin at the aircraft center of gravity, with Z_{EA} along the vertical (positive downward), X_{EA} in the vertical plane containing X_A (positive forward), and Y_{EA} forming a right-hand system.

The Earth-Plane of Symmetry Coordinate System, $X_{E(PS)}$, $Y_{E(PS)}$, $Z_{E(PS)}$ has its origin at the aircraft center of gravity, with $Z_{E(PS)}$ along the vertical (positive downward), $X_{E(PS)}$ in the plane of symmetry (positive forward), and $Y_{E(PS)}$ forming a right-hand system.

The Air Mass Coordinate System, X_{AM}, Y_{AM}, Z_{AM}, is non-rotating with respect to the Earth Coordinate System, with X_{AM} along X_E, Y_{AM} along Y_E, and Z_{AM} along Z_E. The origin of the air mass coordinates translates with the average velocity of the air and coincides with the center of gravity of the aircraft at a particular instant.

The coordinate systems are shown in Fig. A-1 in arbitrary positions. The aircraft axes can be translated from coincidence with the earth axes in an infinite number of ways. One useful method includes yawing about the Z_E axis, elevating about the Y_{EA} axis, and rolling about the X_A axis, giving rise to the angles

$$H = \text{aircraft heading angle} = {}^A[X_E - X_{EA}]$$

$$E = \text{aircraft elevation angle} = {}^A[X_{EA} - X_A]$$

$$\phi = \text{aircraft roll angle} = {}^A[Y_{EA} - Y_A]$$

By the use of angles H, E, and ϕ, the angular orientation of the aircraft is established with respect to the earth. It must be remembered that since large angles cannot be treated as vectors, the rotations must be made in the proper order.

Table A-I: Conversions between Aircraft Coordinate System and Earth Coordinate System using angles H, E, and ϕ.

	R_{X_E}	R_{Y_E}	R_{Z_E}
R_{X_A}	$\cos H \cos E$	$\cos E \sin H$	$- \sin E$
R_{Y_A}	$\cos H \sin E \sin \phi - \sin H \cos \phi$	$\cos H \sin E \sin \phi + \cos H \cos \phi$	$\cos E \sin \phi$
R_{Z_A}	$\cos H \sin E \cos \phi + \sin H \sin \phi$	$\sin H \sin E \cos \phi - \cos H \sin \phi$	$\cos E \cos \phi$

Three other useful angles to relate the Aircraft Coordinate System and the Earth Coordinate System are:

$$\psi = \text{aircraft yaw angle}$$
$$= {}^A[X_E - X_{E(PS)}]$$
$$B = \text{aircraft bank angle}$$
$$= {}^A[Y_{E(PS)} - Y_A]$$
$$\theta = \text{aircraft pitch angle}$$
$$= {}^A[X_{E(PS)} - X_A]$$

Table A-2: Conversions between Aircraft Coordinate System and Earth Coordinate System using angles ψ, B, and θ.

	R_{X_E}	R_{Y_E}	R_{Z_E}
R_{X_A}	$\cos \psi \cos \theta + \sin \psi \sin B \sin \theta$	$\cos \psi \sin B \sin \theta - \sin \psi \cos \theta$	$-\cos B \sin \theta$
R_{Y_A}	$\sin \psi \cos B$	$\cos \psi \cos B$	$\sin B$
R_{Z_A}	$\cos \psi \sin \theta - \sin \psi \sin B \cos \theta$	$-\cos \psi \sin B \cos \theta - \sin \psi \sin \theta$	$\cos B \cos \theta$

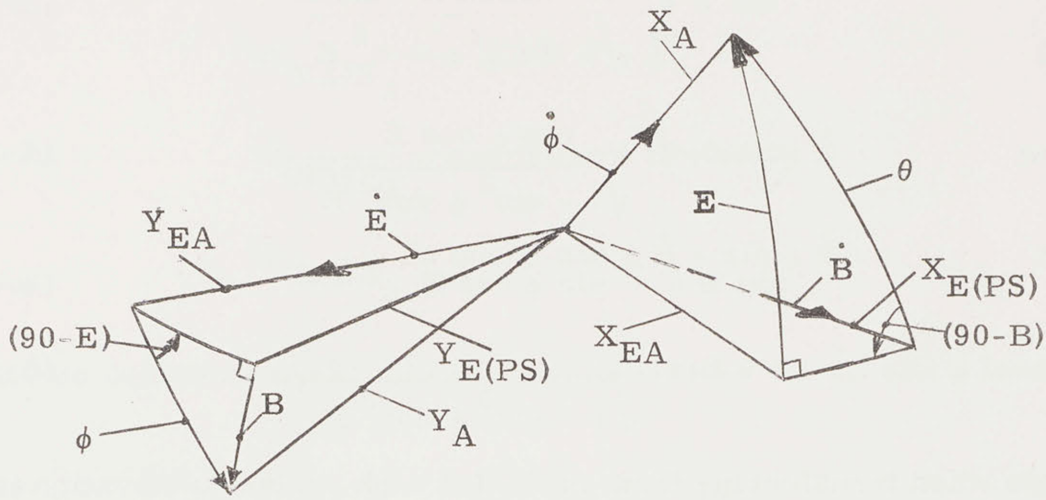

(a) Bank Angle and Roll and Elevation Angles.

It can be seen by use of spherical triginometry that

$$\frac{\sin \phi}{\sin 90} = \frac{\sin B}{\sin (90 - E)}$$

or

$$\sin B = \sin \phi \cos E$$

(b) Elevation Angle and Pitch and Bank Angles.

It can be seen by use of spherical triginometry that

$$\frac{\sin \theta}{\sin 90^{\circ}} = \frac{\sin E}{\sin (90 - B)}$$

or

$$\sin E = \sin \theta \cos B$$

Fig. A-2: Relationship between angles.

The two basic expressions relating the two systems or orientation angles are developed in Fig. A-2. Expanding these two expressions yields

$$\sin\theta = \frac{\sin E}{\sqrt{1 - \sin^2\phi\cos^2 E}} \tag{A-1}$$

$$\cos\theta = \frac{\cos\phi\cos E}{\sqrt{1 - \sin^2\phi\cos^2 E}} \tag{A-2}$$

$$\sin B = \sin\phi\cos E \tag{A-3}$$

$$\cos B = \sqrt{1 - \sin^2\phi\cos^2 E} \tag{A-4}$$

for use when transferring from pitch and bank angles to elevation and roll angles, and

$$\sin E = \sin\theta\cos B \tag{A-5}$$

$$\cos E = \sqrt{1 - \sin^2\theta\cos^2 B} \tag{A-6}$$

$$\sin\phi = \frac{\sin B}{\sqrt{1 - \sin^2\theta\cos^2 B}} \tag{A-7}$$

$$\cos\phi = \frac{\cos\theta\cos B}{\sqrt{1 - \sin^2\theta\cos^2 B}} \tag{A-8}$$

for use when transferring from elevation and roll angles for pitch and bank angles.

The maneuvering aircraft has components of angular velocity about all three body axes. The vector sum of these components is the angular velocity of the aircraft, which is denoted by $\overline{W}_{EA}$ when measured with respect to the earth. The aircraft angular velocity gives rise to rates of change of the orientation angles. It can be seen from Fig. A-1 that

1. $\dot{H}$ is about Z_E
2. $\dot{E}$ is about Y_{EA}
3. $\dot{\phi}$ is about X_A

and consequently these angular velocities are not mutually orthogonal. However, these angular velocities are independent, and hence their vector sum must equal $\overline{W}_{EA}$. Projecting these angular velocities onto aircraft axes gives

$$W_{(EA)X_A} = -\sin E\,\dot{H} + \dot{\phi} \qquad \text{(A-9)}$$

$$W_{(EA)Y_A} = \cos E \sin \phi\,\dot{H} + \cos \phi\,\dot{E} \qquad \text{(A-10)}$$

$$W_{(EA)Z_A} = \cos E \cos \phi\,\dot{H} - \sin \phi\,\dot{E} \qquad \text{(A-11)}$$

Solving equations (A-9), (A-10), and (A-11) for $\dot{H}$, $\dot{E}$, and $\dot{\phi}$ leads to

$$\dot{H} = \frac{\sin \phi}{\cos E} W_{(EA)Y_A} + \frac{\cos \phi}{\cos E} W_{(EA)Z_A} \qquad \text{(A-12)}$$

$$\dot{E} = \cos \phi\, W_{(EA)Y_A} - \sin \phi\, W_{(EA)Z_A} \qquad \text{(A-13)}$$

$$\dot{\phi} = W_{(EA)X_A} + \tan E \sin \phi\, W_{(EA)Y_A} + \tan E \cos \phi\, W_{(EA)Z_A} \qquad \text{(A-14)}$$

The integration of equations (A-12), (A-13), and (A-14) yields the aircraft orientation, given its angular velocity in aircraft coordinates.

From Fig. A-1, it can be seen that

1. $\dot{\psi}$ is about Z_E
2. $\dot{B}$ is about $X_{E(PS)}$
3. $\dot{\theta}$ is about Y_A

It is useful to express the relationship between the rates of roll, pitch and yaw and the rates of change of the yaw, bank, and pitch orientation angles. Projecting these orientation rates onto aircraft axes gives

$$W_{(EA)X_A} = \dot{B} \cos \theta - \dot{\psi} \cos B \sin \theta \qquad \text{(A-15)}$$

$$W_{(EA)Y_A} = \dot{\theta} + \dot{\psi} \sin B \tag{A-16}$$

$$W_{(EA)Z_A} = \dot{\psi} \cos B \cos \theta + \dot{B} \sin \theta \tag{A-17}$$

Solving equations (A-15), (A-16) and (A-17) for the orientation rates leads to

$$\dot{\psi} = - \frac{\sin \theta}{\cos B} W_{(EA)X_A} + \frac{\cos \theta}{\cos B} W_{(EA)Z_A} \tag{A-18}$$

$$\dot{B} = \cos \theta \; W_{(EA)X_A} + \sin \theta \; W_{(EA)Z_A} \tag{A-19}$$

$$\dot{\theta} = \tan B \sin \theta \; W_{(EA)X_A} + W_{(EA)Y_A} - \tan B \cos \theta \; W_{(EA)Z_A} \tag{A-20}$$

In the fixed-gun interceptor aircraft, the controlled line is fixed to the aircraft, hence the angular velocity of the controlled line with respect to the earth is identical with the angular velocity of the aircraft with respect to the earth.

APPENDIX B

COMPUTER AND RADAR COORDINATE SYSTEMS

In a closed loop tracking system, the tracking line is maintained along the line of sight by proper control of the aircraft. The tracking inaccuracy is detected by the radar, and a tracking correction signal is transmitted to the controls. The prediction is based on the motion required of the aircraft in the process of tracking. The output signal from the prediction computer is used to displace the tracking line with respect to the aircraft.

The computer axes for a closed-loop Fire Control System are fixed to the aircraft with the controlled line forward, the elevation axis along the Y_A axis, and the deflection axis forming a right-hand system. The controlled line is not always aligned with the X_A axis, for at different speeds and altitudes the trim angle of attack varies, and, as a result, the X_A axis is reorientated with respect to the aircraft. Fig. B-1 shows the relationship between computer and aircraft coordinates for a closed loop tracking system.

Fig. B-1 was drawn with no aerodynamic yaw existing. Positive aerodynamic yaw occurs when controlled line or nose of the aircraft turns clockwise about the Z_A axis away from the velocity vector. In terms of the notation used in this analysis, $\alpha_{(CL)_e}$ is the angle of attack of controlled line represented as a vector along the Y_A axis, and $\alpha_{(CL)_d}$ is angle of aerodynamic yaw represented as a vector along Z_A axis. In the analysis conducted here, it was assumed that no aerodynamic yaw existed; hence $\alpha_{(CL)_d} = 0$. It was seen from Fig. B-1 that the elevation component of an angle measured in computer

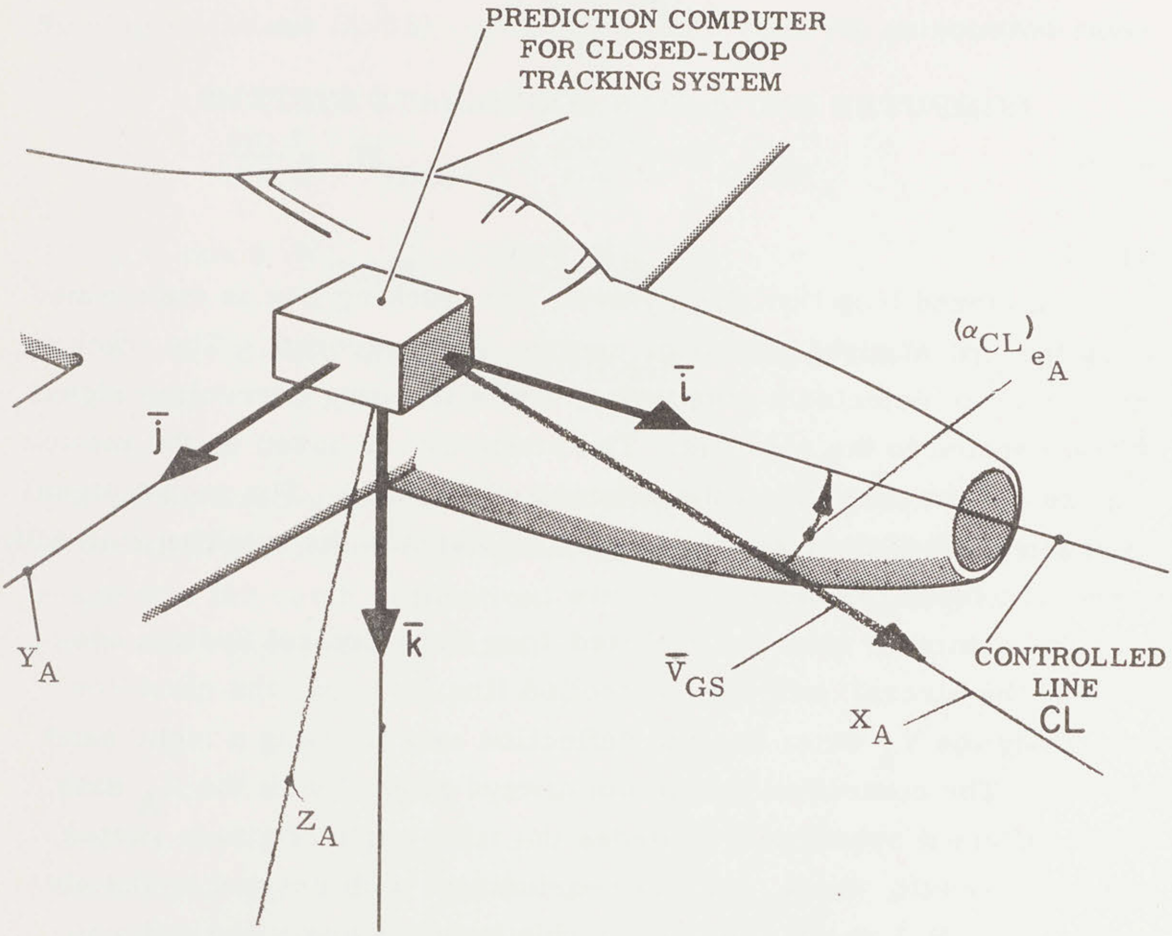

FROM "T-10"

For the purposes of this analysis it was assumed that no aerodynamic yaw existed.

$\bar{i}$ = unit vector along controlled line.

$\bar{j}$ = unit vector along elevation axis of computer.

$\bar{k}$ = unit vector along deflection axis of computer.

Fig. B-1 -Relationship between computer and aircraft coordinates for a closed-loop tracking system.

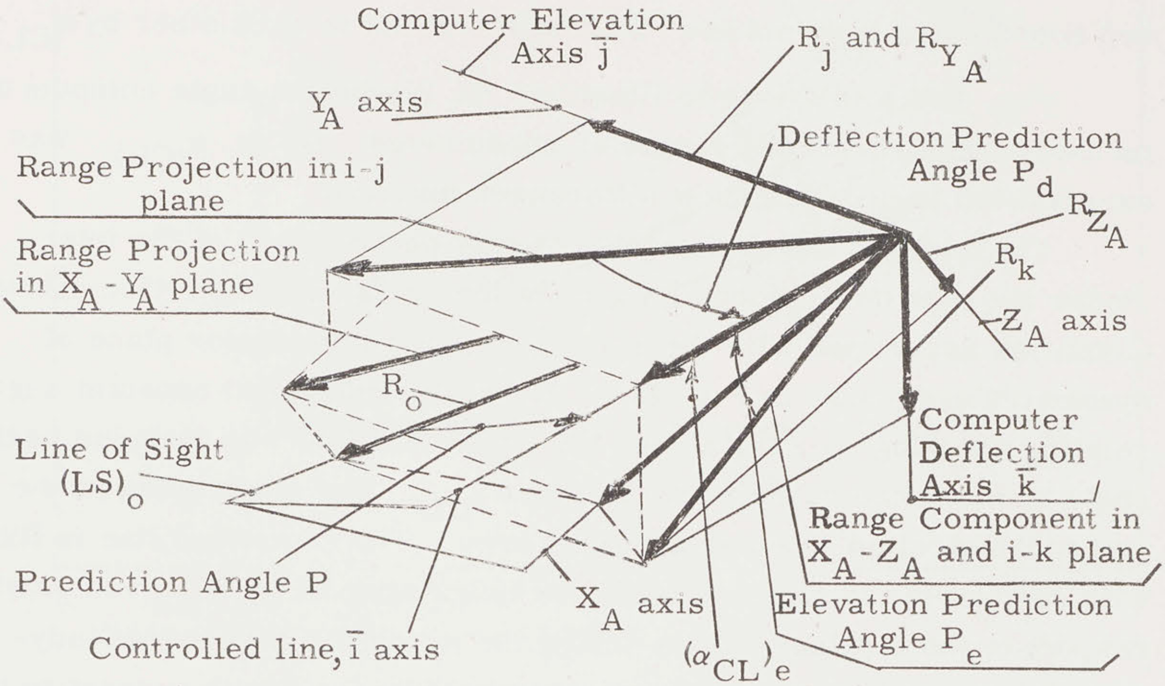

In the diagram: Aerodynamic yaw assumed zero

$$\tan P_e = \frac{R_k}{R_i} \;;\quad \tan P_d = \frac{-R_j}{R_i} \;;\quad \cos P = \frac{R_i}{R_o}$$

$$P_e = (\alpha_{CL})_e + \tan^{-1}\frac{R_{Z_A}}{R_{X_A}} \;;\quad \tan P_d = -\frac{R_{Y_A}}{R_{X_A}}$$

Fig. B-2 Diagram showing Prediction angle components in computer and aircraft coordinates.

coordinates was less by $\alpha_{(CL)_e}$ than the same angle measured in aircraft coordinates. The deflection component of an angle measured in computer coordinates is related to the deflection component measured in aircraft coordinates by cos $(\alpha_{(CL)_e}$ since the deflection axis of the two coordinates systems are tilted with respect to each other by $\alpha_{(CL)_e}$.

Fig. B-2 was drawn to illustrate the prediction angle components measured in aircraft and computer coordinates. Here, $\alpha_{(CL)_e}$ was exaggerated in order to show differences involved.

The angle of attack depends not only on the speed of the interceptor but also on its normal acceleration or "g-loading". Geometrical quantities associated with the quantities in the interceptor plane of symmetry are shown in Fig. B-3. Here, the additional constant angle relating the wing no-lift line and the controlled line was included as the angle of incidence of the controlled line I_{CL}. The angle between the gun and controlled line was assumed zero. The controlled line is fixed with respect to the airplane while the orientation of the V_{GS} vector with respect to the airplane varies during the pursuit. For level steady-state flight conditions the V_{GS} vector would be fixed with respect to the airplane and would be below the no-lift line of the airplane by α_e, the aerodynamic angle of attack. The no-lift line is a line fixed in the airplane where theoretically no lifting force would be acting on the airplane if V_{GS} were along this line. Lift is proportional to α_e for a given V_{GS} and altitude, and hence in steady-state level flight α_e is constant and just large enough to produce a lift equal to the weight of the airplane. Usually the controlled line is inclined below the no-lift line of the airplane by an amount I_{CL} equal to the high speed angle of attack of the airplane in level flight at sea level.

$$\alpha_e = \alpha_{(CL)_e} - I_{CL} \qquad \text{(B-1)}$$

For the boresighted condition:

$$\alpha_e]_{\text{at } V_{GS_{max}}} = - I_{CL} \qquad \text{(B-2)}$$

$$\alpha_{(CL)_e} = 0 \qquad \text{(B-3)}$$

$$J_e = 0$$

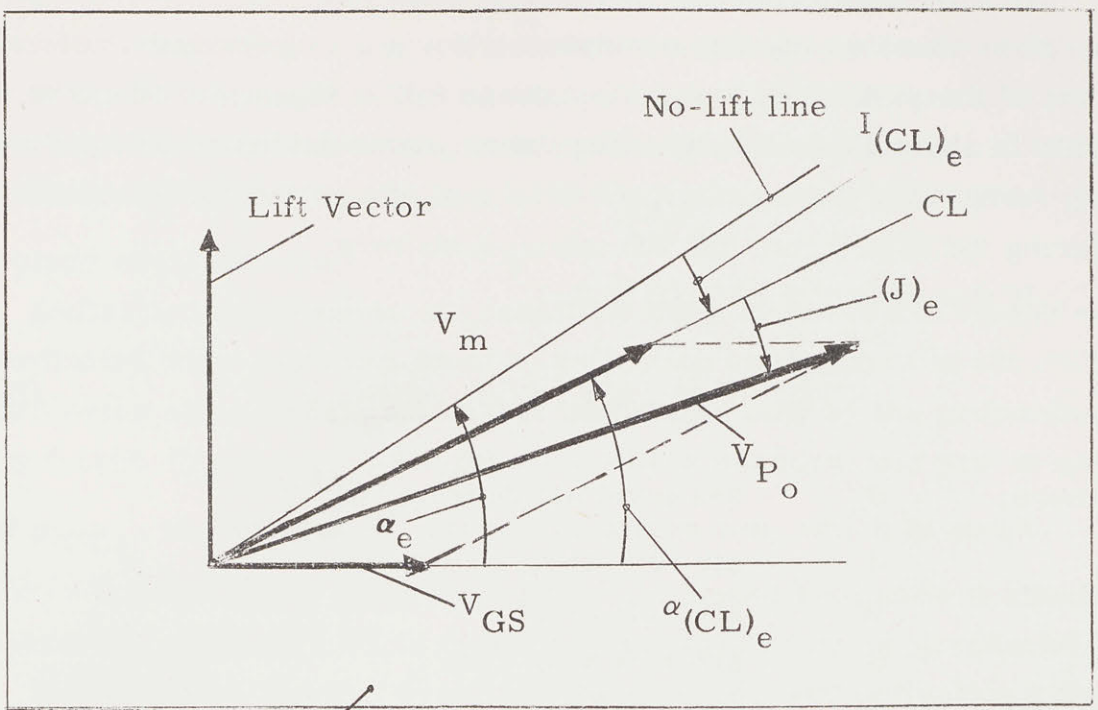

Plane of symmetry of interceptor

From the diagram:

$$\alpha_e = \alpha_{(CL)_e} - I_{(CL)_e}$$

Boresighting is normally performed such that:

$$I_{(CL)_e} = -\alpha_e] \text{ at } (V_{GS})_{max}$$

Hence, when at boresighted conditions of sight:

$$\alpha_{(CL)_e} = 0$$

$$J_e = 0$$

Fig. B-3 Geometrical quantities in interceptor plane of symmetry.

In order to follow a pursuit path of varying curvature, the pursuit airplane must supply the aerodynamic force along the radius of curvature of the path to force the airplane to follow the required curve. This is accomplished by banking the airplane and hence tilting the lifting force toward the center of curvature. Since the curvature varies during the attack run, the lift and α_e also vary.

It was shown in Ref. (1) that:

$$\frac{(\text{lift})}{W} = \frac{d_o}{2} \frac{1}{W/S} \, d/d_o \frac{d_{CL}}{d\alpha_e} \alpha_e \qquad \text{(B-5)}$$

where:

d_o = sea level air density

d = air density at altitude

W = aircraft weight

S = aircraft wing area

$\frac{d_{CL}}{d\alpha_e}$ = rate of change of lift coefficient with angle of attack in plane of symmetry.

Substituting equation (B-1) into (B-5) gives:

$$\frac{(\text{lift})}{W} = \frac{d_o}{2} \frac{1}{W/S} \frac{d}{d_o} \frac{d_{CL}}{d\alpha_e} (\alpha_{(CL)_e} - I_{CL}) \qquad \text{(B-6)}$$

Substituting equation (B-2) into (B-6) gives:

$$\frac{(\text{lift})}{W} = \frac{d_o}{2} \frac{1}{W/S} \frac{d}{d_o} \frac{d_{CL}}{d\alpha_e} (\alpha_{(CL)_e} + [\alpha_e]_{\text{at } V_{GS_{max}}}) \qquad \text{(B-7)}$$

Lift divided by weight is the g-loading on the airplane. It is seen from equation (B-7) that $\alpha_{(CL)_e}$ during the attack depends not only on the change in speed of the interceptor aircraft but also on the g-loading and change of altitude during the attack run*.

---

* In the strictest sense, $\frac{d_{CL}}{d\alpha_e}$ is a variable dependent on Mach Number; and aircraft weight varies continuously during the attack run as fuel is consumed by the interceptor. These effects were not discussed here.

In the equations developed herein for the Attack Simulator, the elevation component of angle of attack was included in the determination of prediction angle. The equations were written in terms of the horizontal and vertical components in Air Mass Coordinates. The deflection component of angle of attack, $\alpha_{(CL)_e}$, (aerodynamic yaw) was assumed equal to zero.

Deflection components of prediction angle measured in computer coordinates were assumed equal to deflection components in aircraft coordinates since it was shown that they differ only by the proportionality factor Cos $(\alpha_{(CL)_e})$ for the case where aerodynamic yaw is zero. For $\alpha_{(CL)_e}$ variation of 10° during the attack run, which is much greater than normally encountered for high speed lead pursuit attacks, a maximum error of 1.5% in deflection measurements is introduced.

In some Fire Control Systems, the elevation and deflection gyros in the computor case are at right angles to each other, with the controlled line perpendicular to the elevation axis but not to the deflection axis due to cross-roll compensation*. Cross-roll considerations were not undertaken here; nor was the attack simulator design undertaken from the design viewpoint of adapting it to a particular fire control system.

In an open-chain tracking system, an attempt is made to separate the functions of tracking and computing. Signals from the tracking inaccuracy detector are transmitted directly to the radar antenna drive to bring the tracking line into coincidence with the line of sight, thus providing a self tracking radar set.

The prediction computer recieves signals proportional to the angular velocity of the tracking line, which with ideal radar equals the angular velocity of the line of sight. The output of the computer is a measure of the desired prediction angle, which is compared with the actual prediction angle as determined by the radar antenna position. The difference between the prediction signals is a measure of the heading error of the aircraft, and consequently is transmitted to the

* See Ref. (3) and Ref. (4) for a more complete discussion of this in connection with the A-1 Sight.

servo system in order that the control surfaces may be appropriately displaced to minimize the error.

The radar tracking line can rotate with respect to the aircraft about two axes. The first, and outer, axis is along $\overline{k}$; the second, and inner, axis is normal to both the $\overline{k}$ axis and the tracking line. These axes are shown in Fig. B-4, together with the input axis for the prediction computer for both the open-chain and closed-loop tracking systems. Unit vectors $\overline{f}$, $\overline{g}$, $\overline{h}$, are selected along the tracking line, the antenna elevation axis, and the open-chain computer deflection axis.

It can be seen that the radar antenna rotates about $\overline{g}$ (the elevation axis of an open-chain system), and $\overline{k}$, the deflection axis of the closed-loop system. It was shown previously that rotations about $\overline{k}$ were essentially equal to rotations about Z_A, the deflection axis of the aircraft. Hence, deflection components measured in radar coordinates are essentially equal to deflection components in aircraft coordinates. However, when prediction angle components are large, trigonometric corrections must be applied about the elevation axis of the radar antenna in order to convert indications to aircraft axis. Once this correction is made in a closed-loop Fire Control System, indications are available for the Attack Simulator in terms of components in Aircraft Coordinates. If the closed-loop Fire Control System does not account for these errors about the elevation axis of the radar, then trigonometric corrections must presumably be made in the Attack Simulator in order to compare the existing signals in radar coordinates with the correct signals in aircraft coordinates as defined by the Attack Simulator.

When prediction angle components are large in open-chain tracking systems, trigonometric corrections must be applied about both the elevation and deflection axis of the open-chain computer. For example, when a deflection prediction angle exists, a correction about $\overline{g}$ axis involves both pitching and rolling of the interceptor aircraft.

It was assumed in the equations set up for the Attack Simulator in this thesis that signals fed back from the Fire Control System and aircraft were available as elevation and deflection components measured

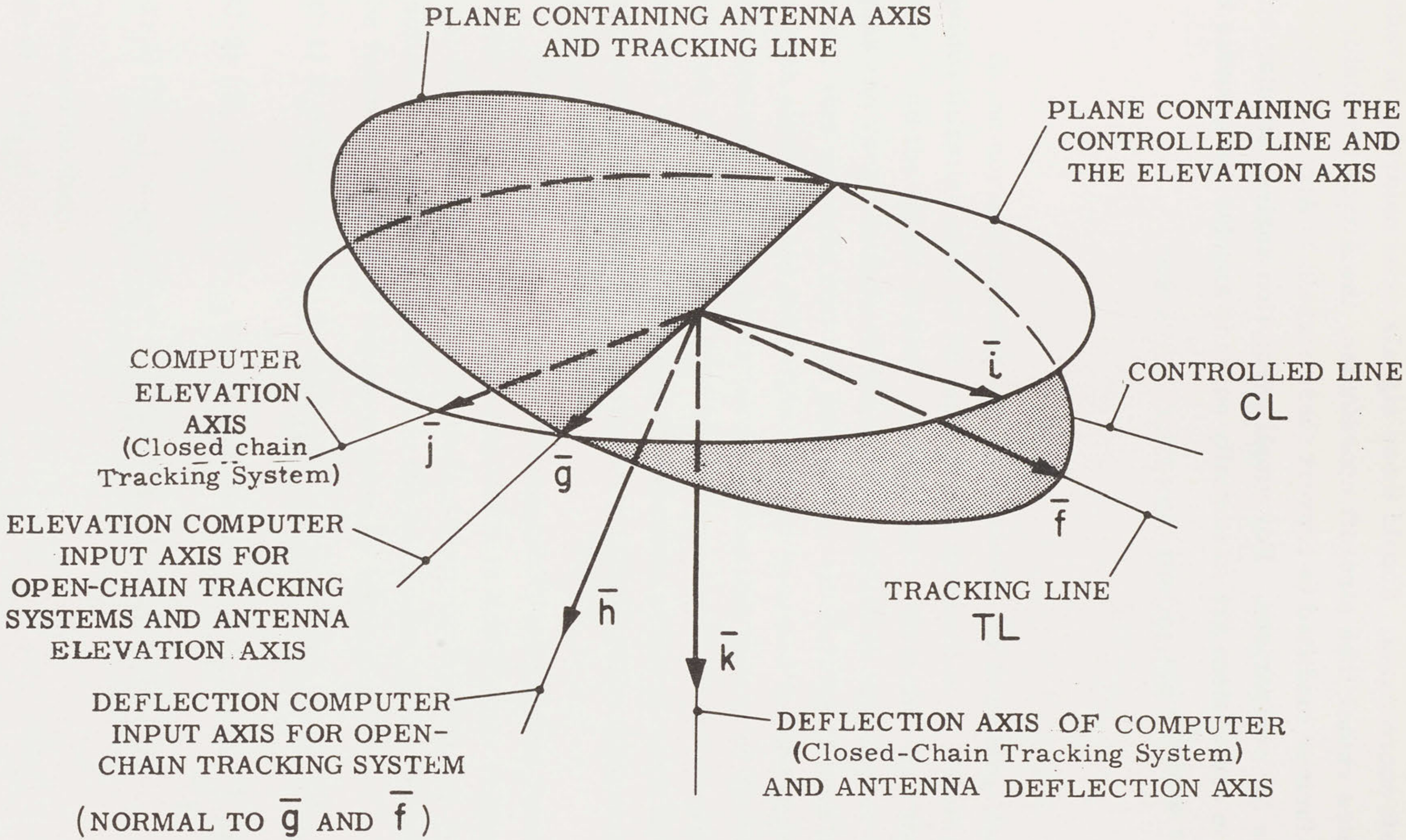

Fig. B-4 Relationship between radar and computer axes for closed-chain and open-chain tracking systems

FROM "T-10

in aircraft coordinates. Should these signals exist naturally in radar coordinates rather than aircraft coordinates, the Attack Simulator must be further modified to convert these signals to Aircraft Coordinates for comparison. For small prediction angles, angular components in one system are essentially equal to angular components in the other system.

APPENDIX C

THE FIRE CONTROL PROBLEM

In the normal tracking control system, the launching line for unguided missiles such as 20 mm cannon projectiles or HVAR rockets must lead the target in both elevation and deflection. For the fixed guns and rocket launchers presently installed in interceptor-type aircraft, this requires that the interceptor aircraft itself lead the target in both elevation and deflection. It was assumed for the purpose of this analysis that the elevation and deflection motion of the interceptor aircraft were uncoupled; that is, the two modes of motion were considered separately. The general response of the aircraft is the superimposed linear sum of its response in the elevation mode and the deflection mode.

The diagram of the three-dimensional Fire Control Problem is shown in Fig. C-1. The only limitation in this picture from any general Fire Control Problem is the fact that, for simplicity, the target motion was restricted to flight in the horizontal plane. From Fig. C-1, the following equations can be written by inspection:

(C-1) $\dot{R}_o = V_T \cos\left[A_{T_o}\right]_h \cos D_{(LS)_o} - V_{GS} \cos (A_{GS})_h \cos (A_{GS})_v$

(C-2) $[W_{LS}]_v = \frac{1}{R_o}\left\{V_{GS} \cos [A_{GS}]_h \sin [A_{GS}]_v - V_T \cos [A_{T_o}]_h \sin D_{(LS)_o}\right\}$

(C-3) $[W_{LS}]_h = \frac{1}{R_o \cos D_{(LS)_o}}\left\{V_T \sin (A_{T_o})_h - V_{GS} \sin (A_{GS})_h\right\}$

It was noted that:

(C-4) $[W_{LS}]_v = \dot{D}_{(LS)_o}$

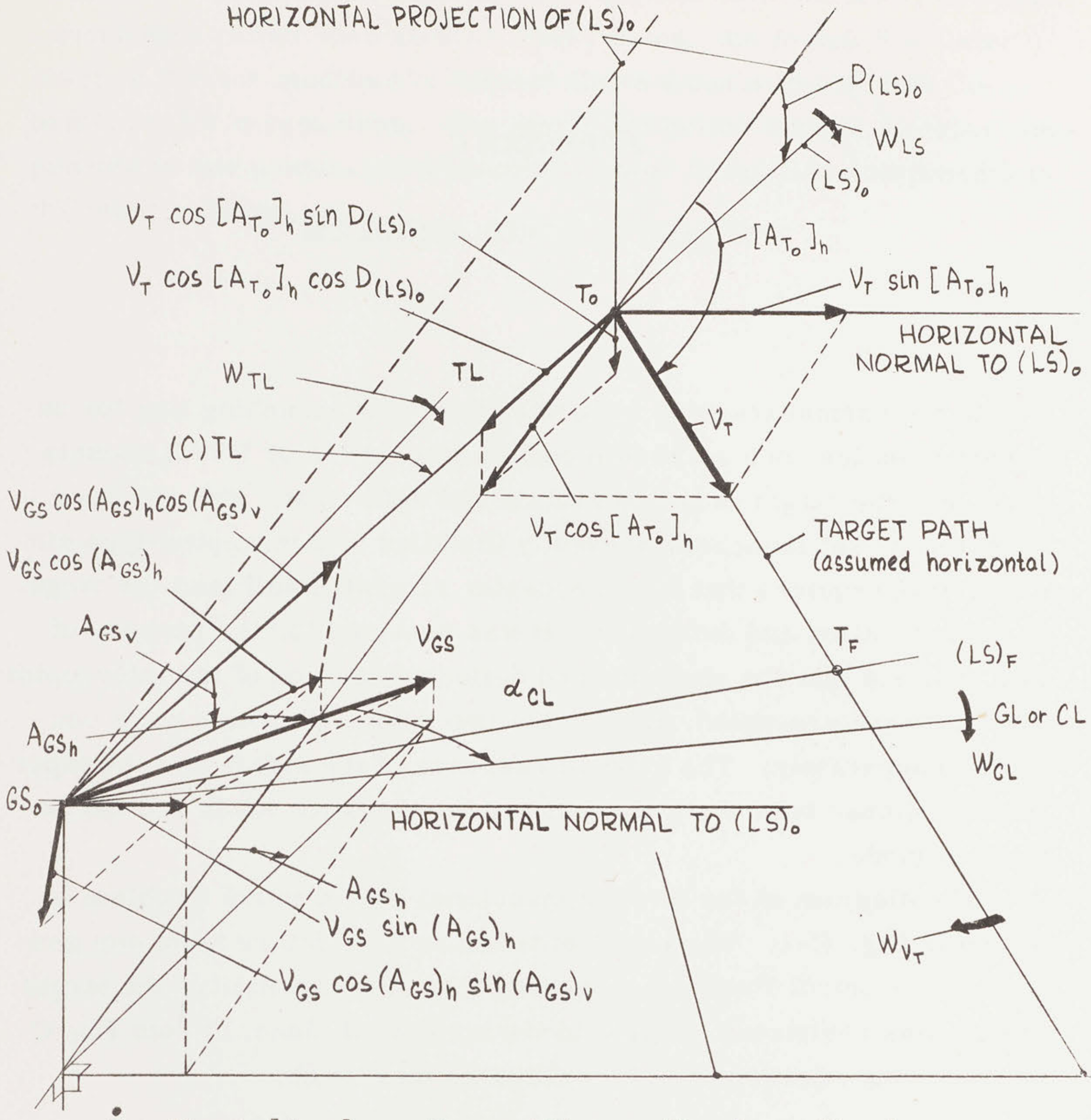

$$\dot{R}_o = V_T \cos [A_{T_o}]_h \cos D_{(LS)_o} - V_{GS} \cos (A_{GS})_h \cos (A_{GS})_v$$

$$[W_{LS}]_v = \frac{1}{R_o}\left\{V_{GS} \cos (A_{GS})_h \sin [A_{GS}]_v - V_T \cos (A_{T_o})_h \sin D_{(LS)_o}\right\}$$

$$[W_{LS}]_h = \frac{1}{R_o \cos D_{(LS)_o}}\left\{ V_T \sin (A_{T_o})_h - V_{GS} \sin (A_{GS})_h \right\}$$

Fig. C-1 Geometry of the fire control problem. Three-dimensional space picture with target path assumed horizontal.

In Fig. C-1, the following quantities were defined:

A. Subscripts:

- $[\ ]_o$ = initial position or initial value.
- $[\ ]_F$ = future position.
- $[\ ]_v$ = vertical component (in Earth Coordinate System)
- $[\ ]_h$ = horizontal component (in Earth Coordinate System)
- $[\ ]_e$ = elevation component (in interceptor A/C coordinates)
- $[\ ]_d$ = deflection component (in interceptor A/C coordinates)

B. Target T:

- A_T = target angle = $A_{(LS-V_T)}$
- A_{V_T} = target course (measured from some horizontal space ref. line to V_T vector).
- V_T = velocity vector of target.

C. Interceptor Aircraft or Gun Station:

- GS = interceptor position
- A_{GS} = interceptor angle = $A_{(LS-V_{GS})}$
- V_{GS} = interceptor velocity vector

D. Space quantities relating target and interceptor:

- R = range
- LS = Line of sight
- $D_{(LS)}$ = Depression of line of sight from horizontal
- TL = Radar tracking line
- CL = Controlled line (assumed coincident with gun line and launching line here)
- C(TL) = Radar tracking line correction
- $W_{(\ )}$ = Angular velocity of ( ).
- α_{CL} = Angle of attack of controlled line $= A_{(V_{GS}-CL)}$

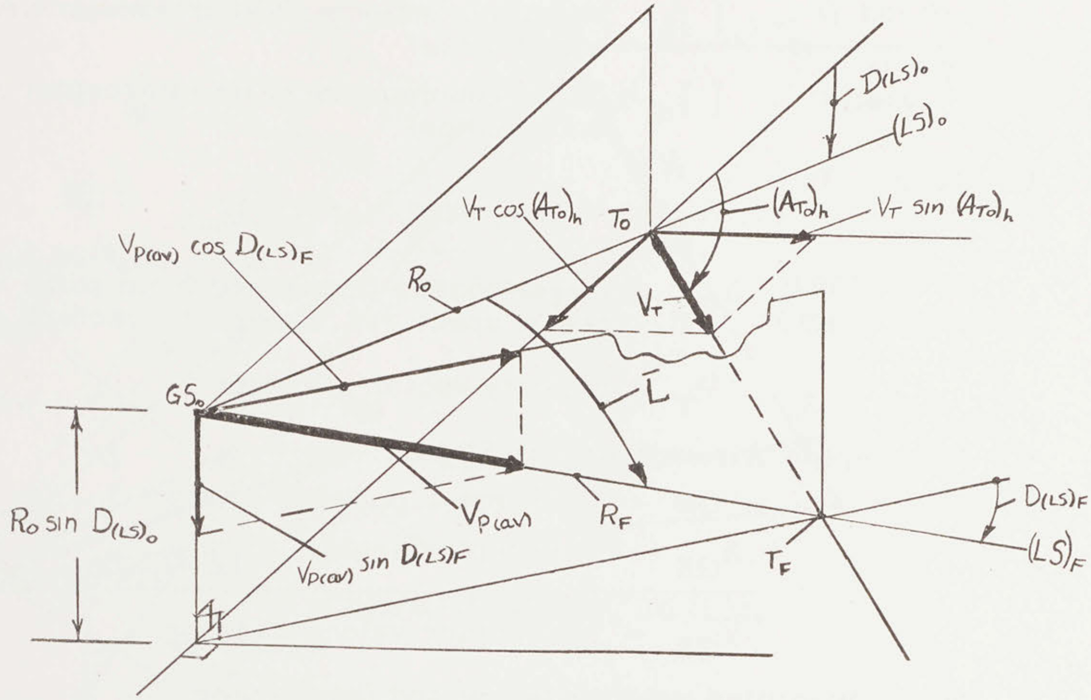

L = Lead Angle = $A_{(LS_o - LS_f)}$

$V_{p(av)}$ = Average Velocity of the Projectile

t_f = Projectile Time of Flight

Fig. C-2 Diagram showing the factors which affect the lead angle.

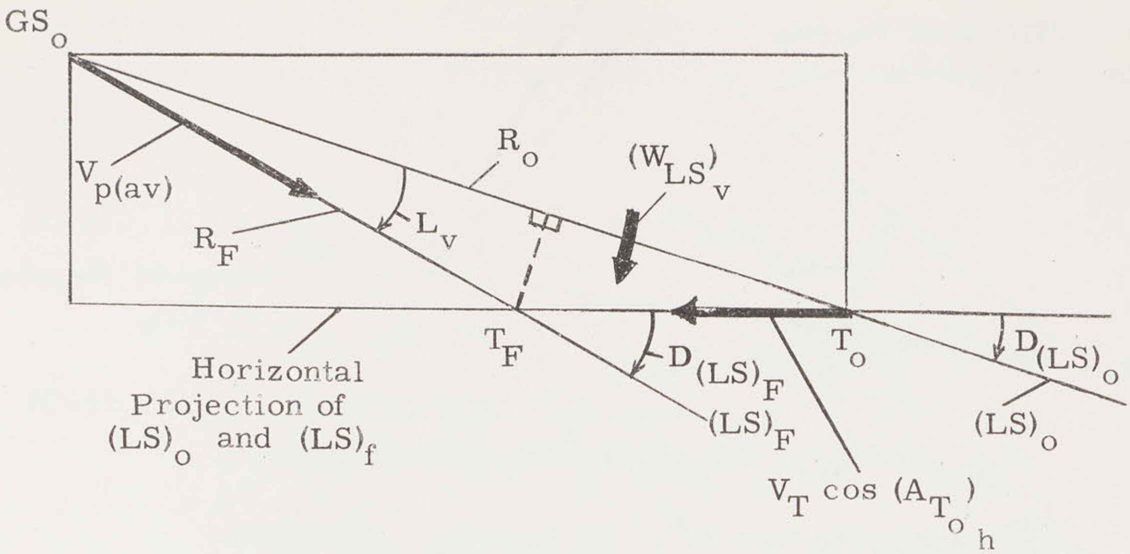

$$V_{p(av)} t_f \sin (L_v) = V_T t_f \cos (A_{T_o})_h \sin D_{(LS)_o}$$

$$\sin L_v = \frac{V_T}{V_{p(av)}} \cos (A_{T_o})_h \sin D_{(LS)_o}$$

For Lead Angle less than 30^o: $\sin L_v \approx L_v$

Therefore:

$$L_v = \frac{V_T}{V_{p(av)}} \cos (A_{T_o})_h \sin D_{(LS)_o}$$

Using the identity:

$$V_{p(av)} = \frac{R_F}{t_f}$$

Vertical component of lead angle may thus be written:

$$L_v = \frac{V_T t_f}{R_F} \cos (A_{T_o})_h \sin D_{(LS)_o}$$

Fig. C-3 Vertical components of lead angle.

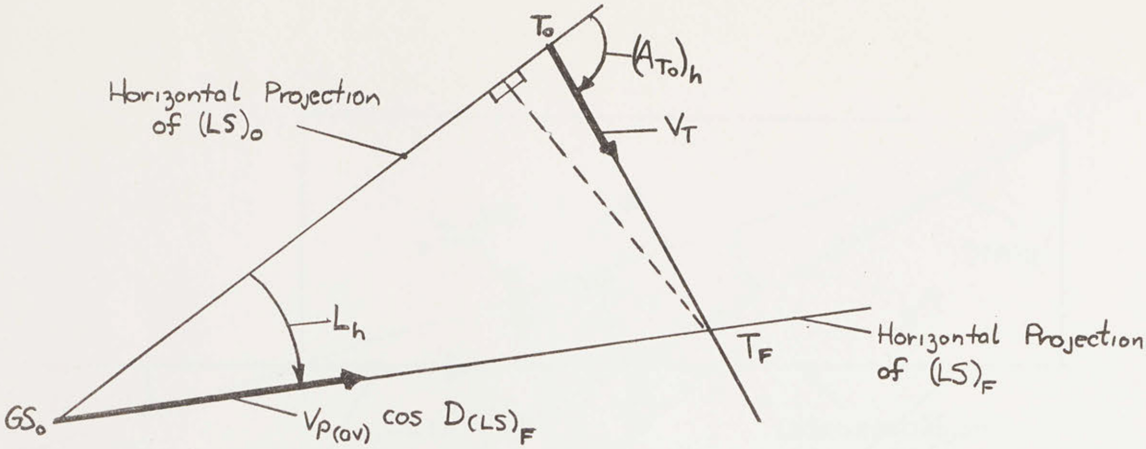

$$(V_{p(av)} \cos D_{(LS)_F})\, t_f \sin L_h = V_T t_f \sin [180-(A_{T_o})_h]$$

For lead less than 30^o, $\sin L_h \approx L_h$, therefore:

$$L_h = \frac{V_T \sin (A_{T_o})_h}{V_{p(av)} \cos D_{(LS)_F}}$$

Using the identities: $V_{p(av)} = \dfrac{R_F}{t_f}$

$$R_F \cos D_{(LS)_f} = \sqrt{R_F^2 - R_o^2 \sin^2 D_{(LS)_o}}$$

an alternate expression is thus:

$$L_h = \frac{V_T t_f \sin (A_{T_o})_h}{\sqrt{R_F^2 - R_o^2 \sin^2 D_{(LS)_o}}}$$

From Fig. C-3 it is seen that:

$$L_v + D_{(LS)_o} = D_{(LS)_F}$$

Another expression for horizontal lead is thus:

$$L_h = \frac{V_T \sin (A_{T_o})_h}{V_{p(av)} \cos (L_v + D_{(LS)_o})}$$

Fig. C-4 Horizontal component of lead angle.

Fig. C-2 was a three-dimensional picture of the factors affecting lead angle. Fig. C-3 considered the vertical plane only and Fig. C-4 the horizontal plane only. From these, the following relations were taken:

(C-5) $$L_v = \frac{V_T t_f}{R_F} \cos (A_{T_{o_h}}) \sin D_{(LS)_o}$$

(C-6) $$L_h = \frac{V_T t_f \sin (A_{T_{o_h}})}{\sqrt{R_F^2 - R_o^2 \sin^2 D_{(LS)_o}}}$$

(C-7) $$L_h = \frac{V_T \sin (A_{T_{o_h}})}{V_{p(av)} \cos (L_v + D_{(LS)_o})}$$

The geometric factors involved in correctly aiming an interceptor aircraft for gunfire or rocket fire were shown in Fig. C-5. The only ballistic affects considered here were those due to gravity drop and velocity jump. From the geometry of Fig. C-5 the following equations resulted:

(C-8) $\overline{P} = \overline{L} + \overline{C} - \overline{J}$

(C-9) $\overline{A}_{GS} = \overline{P} - \overline{\alpha}_{CL}$

(C-10) $(A_{GS})_v = L_v + C - J_v - (\alpha_{CL})_v$

(C-11) $(A_{GS})_v = (P_S)_v - [(C)TL]_v - (\alpha_{CL})_v$

(C-12) $(A_{GS})_h = L_h - J_h - (\alpha_{CL})_h$

(C-13) $(A_{GS})_h = (P_S)_h - [(C)TL]_h - (\alpha_{CL})_h$

A detailed discussion of gravity drop and velocity jump was taken up in Appendix D.

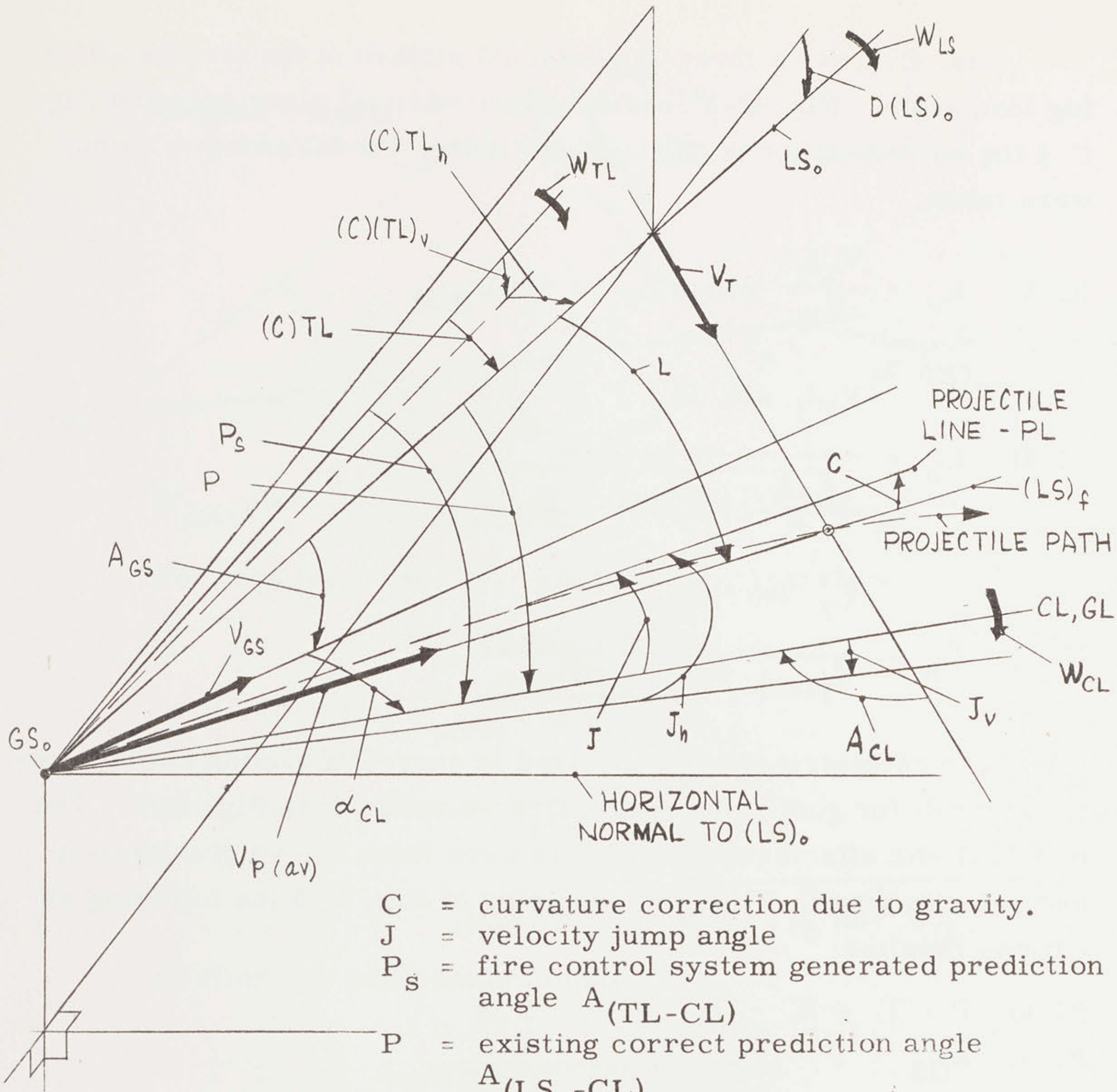

C = curvature correction due to gravity.
J = velocity jump angle
P_s = fire control system generated prediction angle $A_{(TL-CL)}$
P = existing correct prediction angle $A_{(LS_o-CL)}$

Gunline and controlled line were assumed coincident here.

From the geometry above;

$$\overline{P} = \overline{L} + \overline{C} - \overline{J}$$

$$\overline{P}_s = \overline{P} + (\overline{C})TL$$

$$\overline{A}_{GS} = \overline{P} - \overline{\alpha}_{CL}$$

Fig. C-5 Geometric factors involved in correctly aiming an interceptor aircraft for gun fire or rocketfire.

APPENDIX D

GUNFIRE AND BALLISTICS

In the interceptor Fire Control System, aiming corrections are normally applied for the following factors:

(1) Gravity Drop: caused by the fall of the projectile during the time of flight to the target, and occuring in the vertical plane.

(2) Velocity Jump: caused by motion of the gun station, which produces a resultant projectile velocity with respect to the air mass that differs in direction from the direction of the gun line or launcher line.

Gravity Drop

The projectile in free flight, being attracted toward the center of the earth, undergoes a downward acceleration due to gravity. The resultant projectile path has a gravity drop curvature as shown in Fig. D-1. Correction for this gravity drop is made by raising the guns in a plane vertical to the earth. The gravity-drop correction is normally less than 15 mils.

In Fig. D-1, it can be seen that curvature of the projectile path is caused by the component of gravity perpendicular to the gun line. For the fighter flying with wings level, the input to the gravity-drop correction is the acceleration of gravity along the deflection axis of the computer. The correction for gravity-drop, however, is made by raising the guns about the elevation axis. When the fighter flies with wings approximately level, gravity-drop has an elevation component only. When the wings of the fighter are not level, a deflection gravity-drop component exists in addition to the elevation component.

For the times of flight encountered in aerial gunnery, the

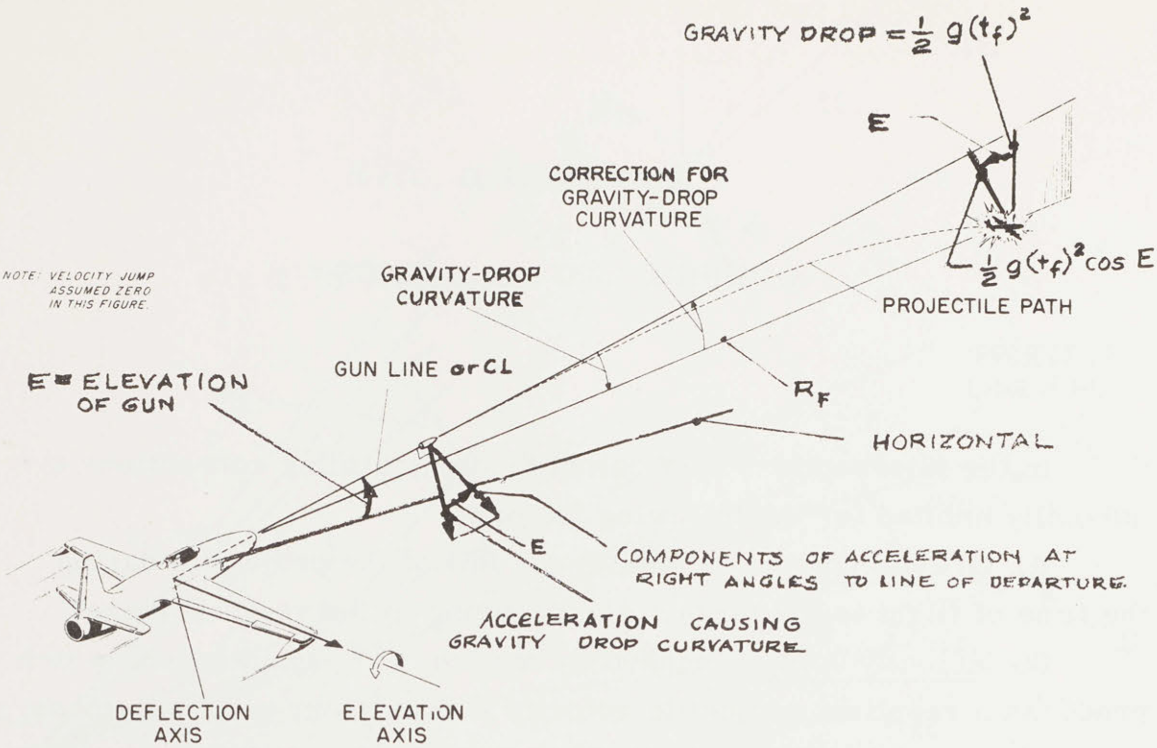

From the figure:

$$\text{Sin}\left[\text{gravity drop angle}\right] = {}^{1}\!/_{2}\ \frac{(g \cos E)\ (t_f^{\,2})}{(\text{av. velocity of proj.})\ (t_f)}$$

t_f = time of flight of projectile from gun to target.

$$\text{Sin C} \simeq C = \frac{1}{2\,V_{p(av)}}\ t_f\ (g \cos E)$$

Fig. D-1 Effect of gravity on the trajectory of a projectile if no air were present gravity drop angle is so small that it differs a negligible amount from its own sine. Under this restriction, the gravity drop angle is equal to the projection of the gravity drop at right angles to the line of departure divided by the slant range. As shown in Fig. D-1, the result is:

$$\text{Sin (Gravity Drop Angle)} = \frac{\frac{1}{2}\ (\text{g Cos E})}{(\text{average vel. of proj.})}\ (t_f) \qquad \text{(D-1)}$$

$$\text{Sin } C \cong C = \frac{1}{2\ V_{p(av)}}\ t_f\ (\text{g cos E}) \qquad \text{(D-2)}$$

or, in another form

$$\text{Sin (Grav. Drop Angle)} = \frac{R_F\ \text{g cos E}}{2\ V_{p(av)}^{2}} \qquad \text{(D-3)}$$

The expression (g Cos E) is the projection of gravity at right angles to the line of departure, so that equation (D-1) may be written:

$$\text{(Grav. Drop Angle)} = \frac{\frac{1}{2}\ (\text{proj. of grav. at rt. angles to gun})}{(\text{av. vel. of projectile})}\ (t_f) \qquad \text{(D-4)}$$

Equation (D-4) shows that the gravity drop angle increases with time of flight, and increases as well with a decrease in the average projectile velocity. This means that the effect of gravity drop is to introduce gravity drop <u>curvature</u> into the trajectory; i.e., the path of the projectile is curved downward away from the line of departure.

The maximum curvature for a given slant range occurs when the projection of gravity at right angles to the gun bore is a maximum; i.e., when the gun is horizontal (E=0). The effect becomes less as this projection decreases until, when the gun is pointed straight up ($E=90^{o}$), no gravity drop angle is present. For intermediate elevation angles, the gravity drop angle for any time of flight and average projectile velocity varies with the cosine of the elevation angle. The gravity drop angle is one of the principle effects taken into account in Fire Control equipment.

Under all circumstances, the force of gravity acts on the projectile in a vertical plane. This means that gravity drop itself can never cause a horizontal displacement of the trajectory.

It is a complex problem to solve equation (D-2) for gravity drop angle, C, due to the difficulty in solving for average projectile velocity and time of flight. The following equations define two different average projectile velocities and the average target velocity.

$$\overline{R}_o = \overline{V}_{p(av)R_o} \, t_{f_o} \qquad \text{(D-5)}$$

$$\overline{R}_F = \overline{V}_{p(av)} \, t_f \qquad \text{(D-6)}$$

$$\text{Target Path from } T_o \text{ to } T_F = \overline{V}_{T(av)} \, t_f \qquad \text{(D-7)}$$

If the projectile is fired to score a hit on a stationary target located at the present target position, the average projectile velocity for the present range, $V_{p(av)R_o}$, and the present time of flight, t_{f_o}, are easily related to the present range and gun station velocity. For this reason, t_{f_o} and $V_{p(av)R_o}$ may be used as basic quantities, although the projectile does not traverse R_o, and t_f differs from t_{f_o}. t_{f_o} is a function of R_o that is given in convenient form in firing tables. It was assumed that the firing tables could be incorporated in a mathematical computer with sufficient accuracy in the ideal Attack Simulator to give $V_{p(av)R_o}$ and t_{f_o} as a continuous output with the computed values of R_o as input.

The gravity drop curvature correction is between the future range vector R_F and controlled line CL. The orientation of C is such that CL is always in the same vertical plane with R_F.

In actual tactical conditions (and hence in the ideal Attack Simulator), the target velocity may change in both magnitude and direction during the time of flight of the projectile. In order to account for this effect, the average target velocity during the time of flight, $V_{T(av)}$, may differ from V_{T_o}, the target velocity vector at the instant of firing. The orientation of the target velocity vector with respect to the present line of sight, $(LS)_o$, is defined by the angles $(A_{T_o})_h$ and $D_{(LS)_o}$. The plane containing the present range vector, the average target motion path, and the future range vector is called the lead plane, because the lead component of the prediction angle is always between two lines in this plane.

The lead plane representation of target angle is the sum of $D_{(LS)_o}$ and $(A_{T_o})_h$, taking into account that these angles are measured in the horizontal and vertical planes respectively. Defining the lead plane target angle as A_{T_L}, from spherical triginometry it may be seen that:

$$\cos (A_{T_L}) = \cos D_{(LS)_o} \cos (A_{T_o})_h \qquad \text{(D-8)}$$

The average value of A_{T_L} between T_o and T_F was denoted by $A_{T_{L(av)}}$.

Lead angle measured in the lead plane is:

$$\cos L = \cos (L_h) \cos (L)_v \qquad \text{(D-9)}$$

or, from Fig. (C-2):

$$\sin L = \frac{V_{T_{(av)}} t_f \sin A_{T_{L(av)}}}{R_F} \qquad \text{(D-10)}$$

The time of flight ratio was defined as:

$$(TFR) = t_f / t_{f_o} \qquad \text{(D-11)}$$

From Fig. (C-2) and equations (D-5) and (D-6), it was seen that:

$$(TFR) = \frac{R_F / V_{p(av)}}{R_o / Vp(av)R_o} = \frac{V_{p(av)R_o}}{V_{p(av)} \cos L - V_{T(av)} \cos A_{T_{L(av)}}} \qquad \text{(D-12)}$$

Substitution of equation (D-11) into equation (D-2) gave:

$$\text{Sin } C = \frac{1}{2 V_{p(av)}} (TFR)\, t_{f_o} \, (g \cos E) \qquad \text{(D-13)}$$

Expanding (TFR) here by equation (D-12) gives:

$$\sin C = (V_{(rel)})\ t_{f_o}\ (g \cos E) \tag{D-14}$$

$$V_{(rel)} = \frac{1}{2}\ \frac{V_{p(av)R_o}}{V_{p(av)}}\ \frac{1}{V_{p(av)} \cos L - V_{T_{(av)}} \cos A_{T_{L(av)}}} \tag{D-15}$$

where $V_{(rel)}$ is the average relative velocity between the target and the projectile projected on $(LS)_o$.

Equations (D-14) and (D-15) define the mathematical equations that the Attack Simulator must solve in order to accurately determine gravity drop. It is seen that these equations are difficult to handle and would require a complex gravity drop computor since $V_{p(av)R_o}$, t_{f_o}, and $V_{p(av)}$ would require a mathematical representation of the Siacci ballistic tables within the computer. All other quantities in these equations are available from the other components of the Attack Simulator or as measured quantities from the interceptor aircraft. Average values of target angle and velocity may be computed during the time of flight of the projectile since their variation with time is programmed in the Attack Simulator.

Since gravity drop seldom exceeds 15 mils in modern interceptor attack problems, it is considered more reasonable for the Attack Simulator to handle this phase of the problem in an approximate manner much the same as the way the latest Fire Control Systems handle it. A complete discussion of gravity drop and how it may be handled with reasonable accuracy by unbalanced mass accelerometers or other means is given in references 3 through 6.

Drift

When a gun is actually fired in the air mass, the projectile does not remain in the vertical plane that contains the line of departure. A horizontal displacement of the point of impact away from the vertical plane containing the gun takes place with respect to the air mass. This effect is drift. Drift is produced by complicated interactions between the gyroscopic momentum of the projectile and the air resistance drag force tangent to the trajectory. If the gun is fired with the bore horizontal, the spin axis of the projectile is initially parallel to the direction of motion, and the center of air resistance is symmetrically located with respect to the body of the projectile. As the projectile moves along the trajectory, the gyroscopic momentum tends to maintain the direction of the long axis unchanged, while gravity drop causes the direction of motion to be altered, so that the center of drag resistance moves from directly on the nose to some position below the nose. The line of action of air drag does not, in general, pass through the center of gravity of the projectile. This means that a torque is set up tending to rotate the projectile about an axis perpendicular to its gyroscopic spin momentum. Under this condition, the spin axis will precess towards the axis about which the torque is applied. As this precession continues, the long axis of the projectile becomes inclined out of the vertical plane containing the line of departure. The resulting attitude of the projectile to the relative wind causes the air drag to set up a force acting to move the projectile in a horizontal direction. The resulting displacement is drift.

Guns are normally rifled so that the projectile spins clockwise, as seen from behind the gun. The corresponding direction of drift is to the right. In practice, the complicated interactions that occur as the projectile continues its flight cause the long axis to vary in direction with respect to the flight path in the manner of a damped oscillation. The corresponding instantaneous values of drift show an oscillatory variation with range, but the net result of the interplay between air drag and gyroscopic action is to cause the projectile to be deflected to the right, out of the vertical plane in which it leaves the gun.

Drift is a maximum when the gun is fired with the bore horizontal. When the gun is fired directly upward, the trajectory is a straight line, so that the resultant force due to air drag remains parallel to the spin momentum of the projectile, and no precessing torque is developed. For gun elevations intermediate between zero and 90 degrees, drift varies with the cosine of the elevation angle. This means that the variation of drift with gun elevation follows the same law as gravity drop. However, the amount of drift is of the order of only 2% of gravity drop. Hence, drift can be neglected as a trajectory factor for the interceptor air-to-air problem.

Velocity Jump

A projectile fired from a moving interceptor enters the air mass with a velocity that is the vector sum of muzzle velocity and interceptor (gun station) velocity. When the gun is pointing in the direction the aircraft is moving, the projectile departs in normal fashion along the gun line, and with a velocity equal to the algebraic sum of interceptor and muzzle velocities. When the angle of attack of the interceptor is increased, the gun line is elevated above the line of aircraft motion and the projectile departs along the projectile line with the resultant projectile velocity the vector sum of muzzle velocity and gun station velocity. The angle measured from the gun line to the projectile line is called velocity jump and is usually from 10 to 40 mils in size. Since the interceptor was assumed in this thesis to be flown without aerodynamic yaw, the velocity jump angle lies in the aircraft plane of symmetry, and only an elevation component exists.

Large angles of attack occur when the fighter flies in a curved path, and it is under this condition that large velocity jump corrections are required. In Fig. D-2 the aircraft is shown pulling out of a dive and undergoing several g's acceleration along the deflection axis. To provide the additional lift required to perform this maneuver, the angle of attack of the aircraft must be increased, placing the gun line above the interceptor velocity vector. Because of the resulting velocity jump, the projectile proceeds along the projectile line which is below the gun line. To correct for this, the gun line must be raised about the elevation axis by the velocity jump correction shown.

The most common maneuver requiring velocity jump correction is the coordinated turn. The turning motion results in a component of centrifugal acceleration along the deflection axis, as well as the component of gravity acceleration. The lift of the aircraft must increase in order to overcome both gravity acceleration and the centrifugal acceleration . To provide the added lift required, the aircraft angle of attack must be increased; to do this, the nose of the interceptor must be raised above the velocity vector. The projectile velocity vector is

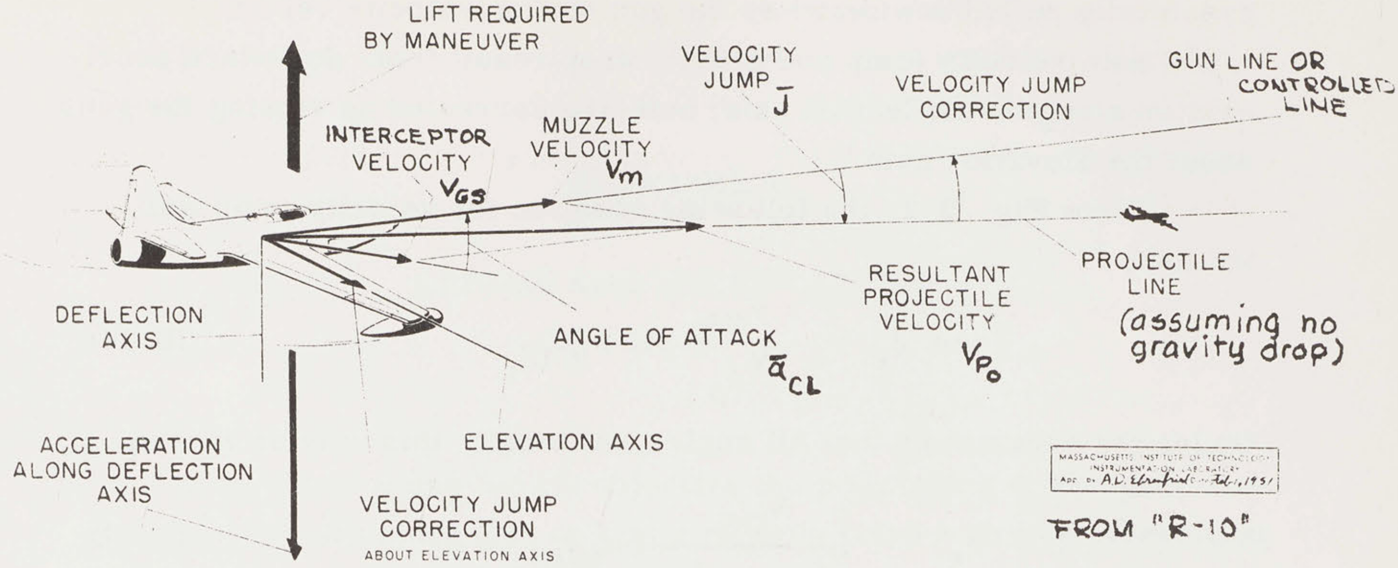

Assuming no aerodynamic yaw, then:

$$\overline{A}_{(CL-V_{GS})} = -\overline{\alpha}_{CL} = -\alpha_{(CL)_e}\,\overline{e} \quad \text{and} \quad \overline{J} = J_e\,\overline{e}$$

$$\sin J_e = \frac{V_{GS}\sin A_{(CL-V_{GS})}}{V_{po}} \quad \text{where} \quad \overline{V}_{po} = \overline{V}_M + \overline{V}_{GS}$$

$$\sin J_e = -\frac{V_{GS}}{V_{po}}\sin \alpha_{(CL)_e}$$

For small angles:

$$J_e \simeq -\frac{V_{GS}}{V_{po}}\,\alpha_{(CL)_e} \simeq -\left(\frac{V_{GS}}{V_M + V_{GS}}\right)\alpha_{(CL)_e}$$

or

$$J_e \approx \left(\frac{V_M}{V_{GS} + V_M} - 1\right)\alpha_{(CL)_e}$$

Fig. D-2 Factors affecting the elevation jump angle of a bullet when fired from an interceptor aircraft.

essentially pulled downward by the gun station velocity vector.

Both velocity jump and gravity drop result from downward acceleration along the deflection axis; both are corrected by raising the guns about the elevation axis.

From Fig. D-2, the following equation for velocity jump was written:

$$\sin J_e = -\frac{V_{GS}}{V_{p_o}} \sin \alpha_{(CL)_e} \qquad \text{(D-16)}$$

Under the assumption that all angles are small, this may be written:

$$J_e \cong -\left(\frac{V_{GS}}{V_M + V_{GS}}\right) \alpha_{(CL)_e} \qquad \text{(D-17)}$$

APPENDIX E

ERRORS AND UNCERTAINTIES

Fire Control has for its objective the positioning on the axis of a gun barrel or launcher line so that a missile fired with this orientation will reach a point in space at the proper time to intercept a target taken under fire. The design of a Fire Control System proceeds from a careful analysis of all the physical factors that can affect the meeting of a projectile and its target. An Attack Simulator that is designed to provide qualitative information on the accuracy of the Fire Control System must be built with even greater regard for the physical factors that act on the missile or projectile.

In a specific gun or projectile, unpredictable departures from the ideal can strongly affect the course of the projectile. Factors of this kind are not within the scope of the Fire Control System to handle. A truly realistic Attack Simulator might consider these departures from ideal by treating them as modifying inputs programmed from statistical information based on accumulated records from actual firing data. When a projectile is fired from an interceptor aircraft, it may miss the target for a variety of reasons. One is the tracking inaccuracy, caused by dynamic lags in the tracking system and by interference effects associated with the radar receiver. Another cause of misses is the inaccuracy of the prediction computer, which may result from either faulty calibration or dynamic effects. In addition, the interceptor aircraft is flying through a turbulent air mass, which causes the controlled line to wander in a random manner. Finally, the projectiles have dispersion with respect to the interceptor aircraft due to imperfections in their manufacture and to the method of firing.

The probability of hitting the vulnerable area of the target depends upon the sum of the inaccuracies. Inaccuracies may be considered to have error components and uncertainty components. The Attack Simulator may provide information on the error components of the Fire Control System solution; the uncertainty components are beyond the capabilities of the Attack Simulator as undertaken in this thesis. Errors are considered to be those components that can be predicted on the basis of static calibration and dynamic analysis. Uncertainties can only be treated statistically.

If the qualitative Attack Simulator were built as an ideal mathematical machine and an attack run was made with it, a time record of controlled line error and future range could be correlated with target size and the rate of fire during the time the pilot simulates firing his guns to give a time record of the miss distance. If the same initial conditions were set up and the same target course and speed were flown by a real target, and if the pilot actually fires his guns during the same time intervals throughout the attack run as in the simulated run, the number of hits scored on the target would differ from the number of hits computed by the Attack Simulator by the factor of uncertainty.

A typical projectile pattern is shown in Fig. E-1. The impact points are the intersections of the projectiles with a plane passing through the center of the target and normal to the line of fire. The center of impact is the average position of all the impact points. The error in the center of impact is the distance from the target to the average position. It was assumed in this thesis that the error in the center of impact was equal to the aiming error of the interceptor aircraft. That is, the error in center of impact was assumed equal to controlled line error.

The scatter of the impact points with respect to the center of impact is commonly measured in terms of the standard deviation. The standard deviation is the root-mean-square of the angular displacement of all the impact points with respect to their average position. When the patters is represented by a Gaussian distribution, 40% of the impact points fall within a circle with radius equal to the standard

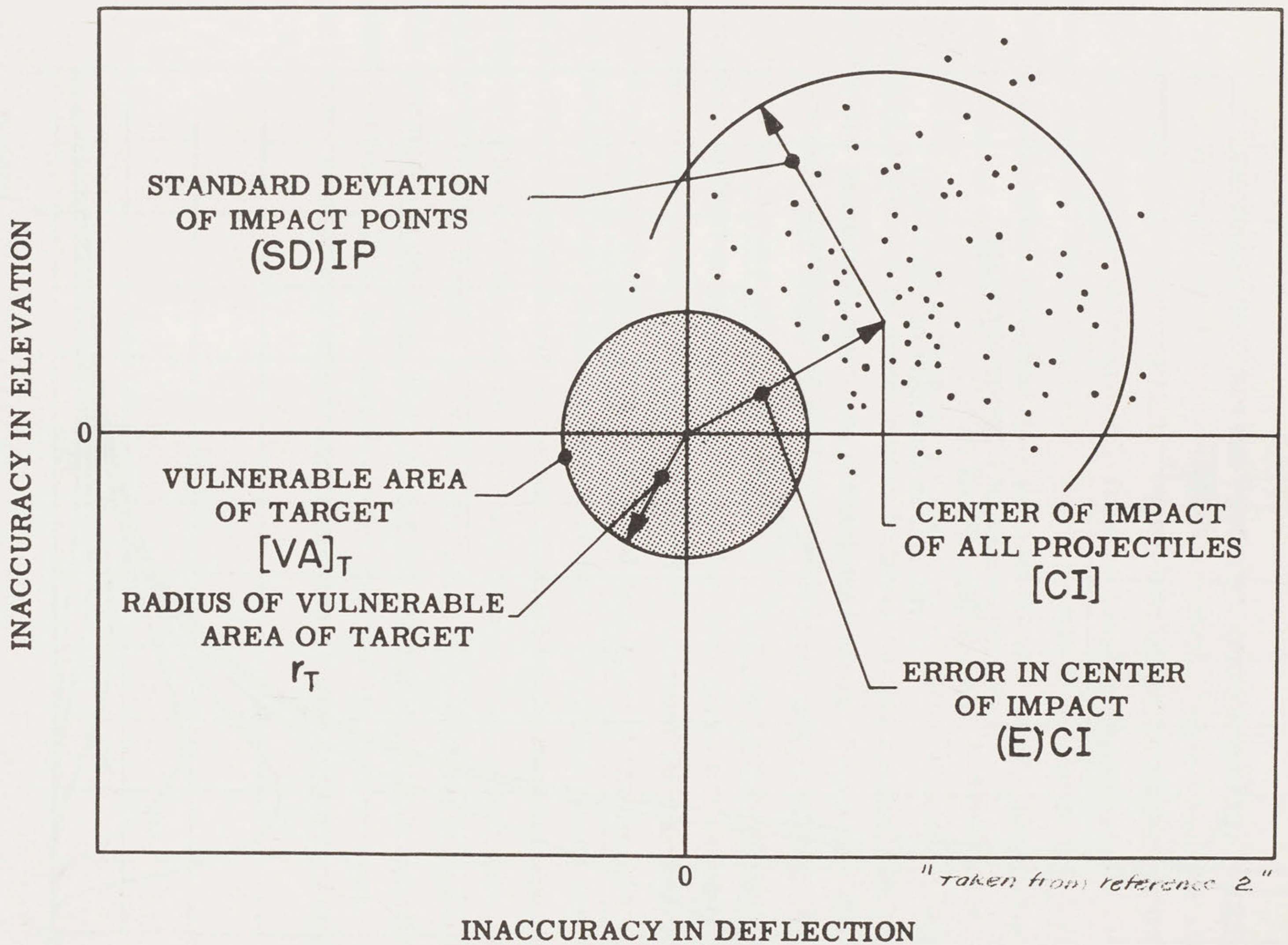

"Taken from reference 2."

FROM "T-10"

Fig.E-1 Impact of projectiles with the plane containing the target and normal to the line of fire.

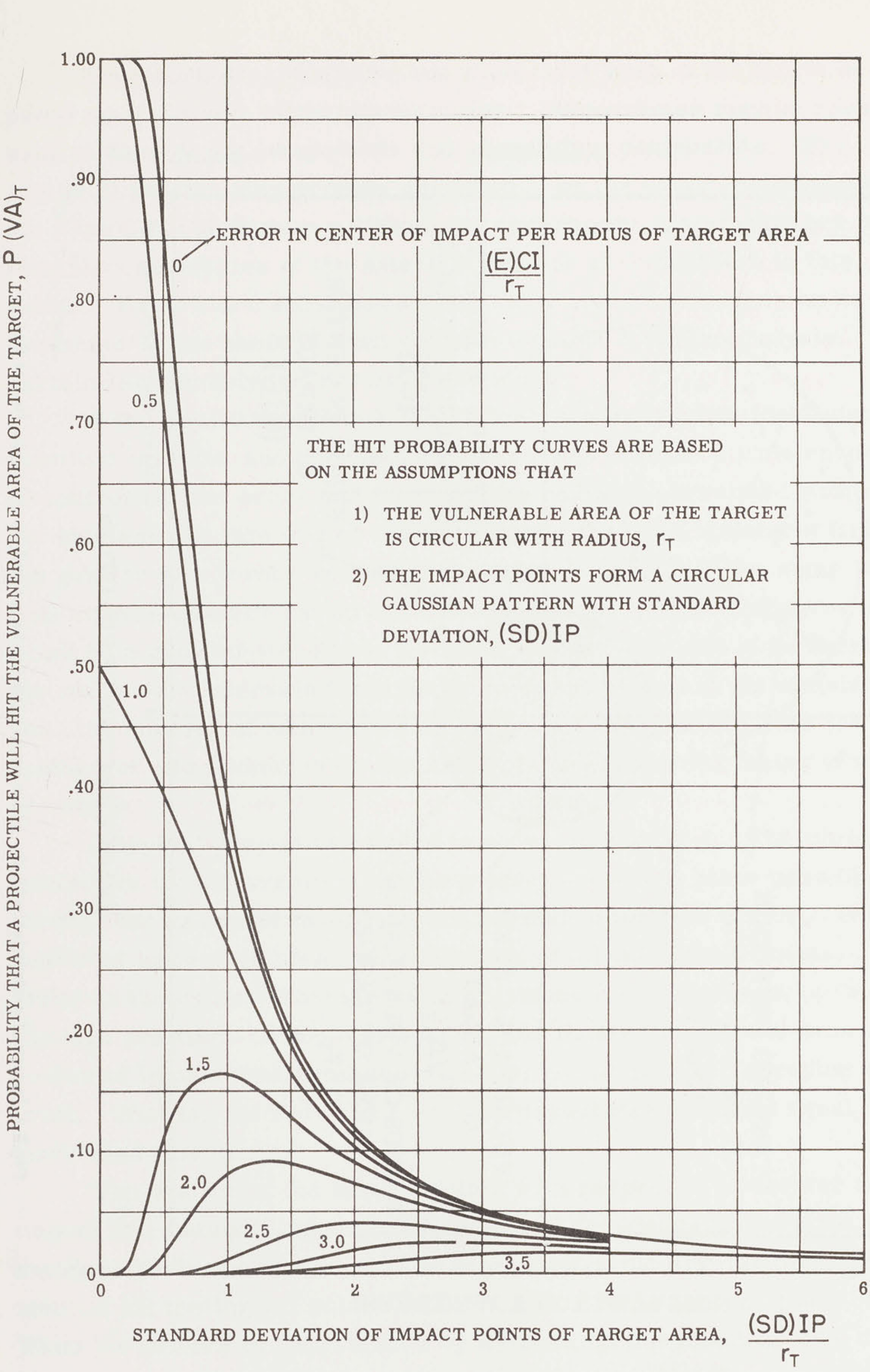

Fig. E-2 Effect of dispersion and aiming error on the probability of a hit.

FROM "T-10"

deviation. The standard deviation results from a random wander of the interceptor due to the effects of gusts and radar interference, and also depends on the dispersion of the projectiles measured with respect to the interceptor.

The probability of hitting the vulnerable area of the target, $P(VA)_T$, depends on the error of the center of impact and the standard deviation of the impact points. When the center of impact is well off the target and the standard deviation is small in comparison with the target radius, there will be a low hit probability, for in this case most of the projectiles will pass by one side of the target. Under the same conditions of center-of-impact error, when the standard deviation is increased, there is increased probability of hits. However, when the standard deviation is much larger than the target radius, the impact points are scattered over a relatively wide area, hence are thinly distributed over the target and the hit probability is decreased. When the error in the center of impact is greater than the target radius, the standard deviation has an optimum value that gives a maximum probability of hit. This is shown in Fig. E-2 in which the hit probability is plotted as a function of the standard deviation of the impact points for various errors in the center of impact. In these plots, the values of standard deviation and error are divided by the target radius in order to non-dimensionalize them and render them applicable to any size of circular target, provided the projectile pattern is Gaussian. For example, from Fig. E-2, it can be seen that, with a non-dimensional error of 2.0, the maximum hit probability is 9 percent. This maximum is achieved with a non-dimensional standard deviation of 1.3.

APPENDIX F

SINGLE-DEGREE-OF-FREEDOM INTEGRATING GYROSCOPE

A complete discussion of the single - degree - of - freedom integrating gyroscope is given in reference 8 of the Bibliography. A simple line drawing of the single - degree - of - freedom gyro is shown in Fig. F-1. A very brief summary of the operation of this unit is given in the following paragraph.

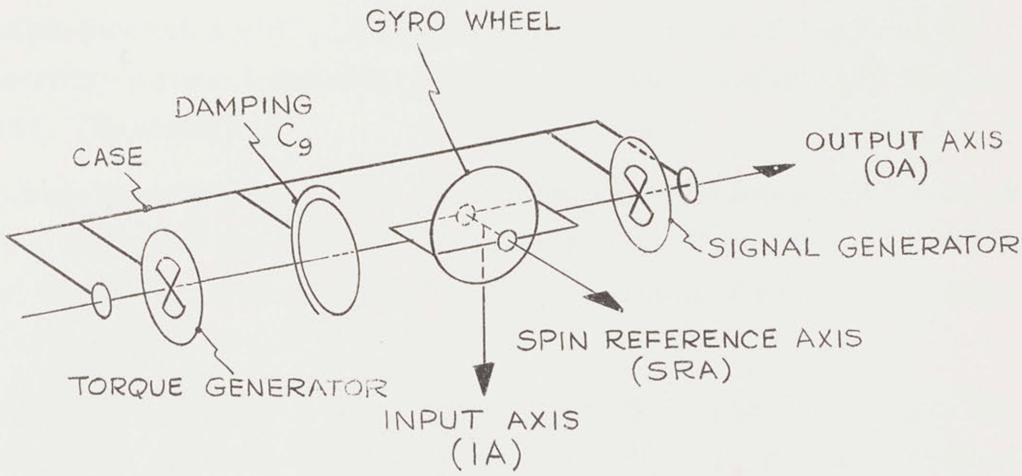

Fig. F-1 Single-degree-of-freedom gyroscope

The torque from the single - degree - of - freedom gyro wheel in an integrating gyro unit is opposed by the torque from a damper. In an ideal situation, the torque from the gyro is proportional to angular velocity around the input axis, and the torque from the damper is proportional to the angular velocity of the output axis with respect to the case. In the steady-state condition when the two torques are equal, the angular velocity of the output axis with respect to the case is proportional to the angular velocity of the case around the input axis. Therefore, the angle of the output axis is proportional to the time integral of the input angular velocity.

A Microsyn may be mounted on the shaft of the output axis; a voltage would be produced that is proportional to the angle turned about the output axis. This voltage is therefore proportional to the time integral of the input angular velocity.

APPENDIX G

REFERENCES AND BIBLIOGRAPHY

1. Perkins, C.D. and Hage, R.E.: "Airplane Performance Stability and Control". John Wiley and Sons, Inc., New York, 1950.

2. Seamans, R.C., Jr. "Comparison of Automatic Tracking Systems for Interceptor Aircraft". Massachusetts Institute of Technology Instrumentation Laboratory, Report T-10; Cambridge, Mass., 1951. (Confidential)

3. Ehrenfried, A.D. "General Operating Principles of the A-1 Gun-Bomb-Rocket Sight". Massachusetts Institute of Technology Instrumentation Laboratory, Report R-10; Cambridge, Mass., 1951. (Restricted)

4. Massachusetts Institute of Technology Instrumentation Laboratory: "A-1 Sight for the Control of Gunfire from Fixed Guns, Rocketfire, and Bombing from Aircraft". Two Volumes, Cambridge, Mass., 1946. (Restricted)

5. NAVORD REPORT 3-47; "Gunsight Mark 15 for the Control of Short and Medium-Range Antiaircraft Fire from Naval Vessels". Vols I and II. Prepared by Massachusetts Institute of Technology Instrumentation Laboratory; Cambridge, Mass., 1947. (Confidential)

6. King, L.H. "Configuration and Dynamics of the Dummy-Gun Fire Control System". Massachusetts Institute of Technology Instrumentation Laboratory, Report R-49; Cambridge, Mass. 1953. (Confidential)

7. Seamans, R.C. and Whitaker, H.P.; "Dynamic Performance of Aircraft Tracking Systems". Tracking Control Progress Report No. 6445-P-5. Massachusetts Institute of Technology Instrumentation Laboratory, Cambridge, Mass. 1948. (Confidential)

8. Jarosh, J.J.; Nugent, J.B.; Meyers, J.S.; Henderson, R.S.; and Hoag, D.G.: "Single-Degree-of-Freedom Integrating Gyro Units for Use in Fire Control Systems". Report R-2, Instrumentation Laboratory, Massachusetts Institute of Technology, Cambridge, Mass., 1952. (Confidential)

9. Hume, E.L.; "Illustrative Analysis of a Single-Axis Support Motion Isolation System Using a Single-Degree-of-Freedom Integrating Gyro Unit as an Angular Deviation Receiver". Report R-7, Instrumentation Laboratory, Massachusetts Institute of Technology, Cambridge, Mass. 1951.